

**RIGA TECHNICAL UNIVERSITY**

Faculty of Materials Science and Applied Chemistry  
Institute of General Chemical Engineering

**Līga STĪPNIECE**

Doctoral student of the programme “Materials Science”

**DEVELOPMENT OF MAGNESIUM MODIFIED  
CALCIUM PHOSPHATE BIO-CERAMIC  
FOR BONE TISSUE REGENERATION**

**Summary of the Doctoral Thesis**

Scientific Supervisors:

Professor, *Dr. sc. ing.* L. BĒRZIŅA-CIMDIŅA

Leading researcher, *Dr. sc. ing.* K. ŠALMA-ANCĀNE

**RTU Press  
Riga 2016**

Stīpniece L. Development of Magnesium Modified Calcium Phosphate Bioceramic for Bone Tissue Regeneration. Summary of the Doctoral Thesis. -R.: RTU Press, 2016. – 35 p.

Printed in accordance with RTU Resolution of the Institute of General Chemical Engineering as of 28 June 2016, Minutes No.16-15/16.

**ISBN 978-9934-10-880-8**

**THE DOCTORAL THESIS PROPOSED TO  
RIGA TECHNICAL UNIVERSITY  
FOR THE PROMOTION TO THE SCIENTIFIC DEGREE  
OF DOCTOR OF ENGINEERING SCIENCES**

To be granted the scientific degree of Doctor of Engineering Sciences, the present Doctoral Thesis is to be publicly defended on 14 December 2016, at the Faculty of Material Science and Applied Chemistry, Riga Technical University, 3 Paula Valdena Str., Room 272 at 1 p.m.

**OFFICIAL REVIEWERS**

Professor, *Dr. sc. ing.* Remo Merijs-Meri  
Institute of Polymer Materials, Riga Technical University

Professor, *Dr. med.* Juta Kroiča  
Department of Biology and Microbiology, Riga Stradins University

Professor, *PhD.* Bikramjit Basu  
Department of Materials Science and Engineering, Indian Institute of Technology, IIT  
Kanpur, India

**DECLARATION OF ACADEMIC INTEGRITY**

I hereby declare that the Doctoral Thesis submitted for consideration to Riga Technical University for promotion to the scientific degree of Doctor of Engineering Sciences is my own and does not contain any unacknowledged material from any source. I confirm that the Doctoral Thesis has not been submitted to any other university for the acquisition of a scientific degree.

Līga Stīpniece .....

Date: .....

The Doctoral Thesis has been written in Latvian and consists of 141 pages. The Thesis contains 3 chapters, *i.e.*, Review of Literature (5 sections), Materials and Methods (4 sections), Results and Discussions (3 sections), as well as Conclusions and a list of References comprising 224 information sources. The Doctoral Thesis has been illustrated by 48 figures and 22 tables.

## ACKNOWLEDGEMENTS

I would like to express the deepest gratitude to the scientific supervisors – *Dr. sc. ing.* Līga Bērziņa-Cimdiņa and *Dr. sc. ing.* Kristīne Šalma-Ancāne – for providing a theoretical background and consultations in order to successfully perform determined tasks, as well as their unselfish support and trust throughout the development of the Doctoral Thesis.

Thanks to a friendly and amenable team of RTU Institute of General Chemical Engineering, Rudolfs Cimdins Riga Biomaterials Innovation and Development Centre for cooperation and assistance. I would like to say special thanks to *Dr. sc. ing.* Jānis Ločs and *Dr. sc. ing.* Dagnija Loča for sharing their experience, advice and recommendations.

Also, I would like to thank the team of the Cell Transplantation Centre of Pauls Stradins Clinical University Hospital, as well as *Dr. Olafur E. Sigurjonsson* (The Blood Bank, Landspítali University Hospital, Iceland) for a possibility to perform the microbiological experiments.

I would like to express the sincerest gratitude to my relatives and friends for motivation, inexhaustible understanding and immeasurable support during my PhD studies.

## CONTENTS

OVERVIEW OF THE DOCTORAL THESIS.....	6
Topicality.....	6
The Aim of the Doctoral Thesis.....	6
Tasks of the Doctoral Thesis.....	6
Thesis Statements.....	7
Scientific Significance.....	7
Practical Significance.....	7
Approbation of Research Results and Publications.....	7
List of Publications.....	8
Participation in the Scientific Conferences.....	9
LITERATURE REVIEW.....	13
EXPERIMENTAL PROCEDURE.....	15
1. Synthesis of Mg-Modified CaP Bioceramic Precursor Powders.....	15
2. Preparation of Mg-Modified CaP Bioceramics.....	16
3. Characterization Techniques.....	16
4. <i>In Vitro</i> Tests of Bioceramics.....	17
RESULTS AND DISCUSSION.....	18
1. Characterisation of Mg-Modified CaP Precursor Powders.....	18
2. Characterisation of Mg-modified HAp Bioceramics.....	20
3. Characterisation of Mg-Modified $\beta$ -TCP Bioceramics.....	23
4. Characterisation of Mg-Modified BCP Bioceramics.....	26
5. Solubility, <i>In Vitro</i> Bioactivity and Cytotoxicity of Mg-Modified CaP Bioceramics.....	28
CONCLUSIONS.....	34
REFERENCES.....	35

## OVERVIEW OF THE DOCTORAL THESIS

### Topicality

According to the reports of the international experts published in the medicine journal *The Lancet* (15 December 2012), musculoskeletal infirmities are among the most disabling and costly conditions affecting hundreds of millions of people around the world. On the basis of these considerations, the regeneration and reconstruction of the bone tissue lost due to fractures, bone infections, tumours, and other disorders or traumatic events represent a major clinical challenge. Thus, the demand for materials to improve the quality of life concerns the specially designed biomaterials for the repair and reconstruction of diseased or damaged hard tissues.

Calcium phosphates (CaP) constitute an inorganic mineral phase in mammalian bones and teeth. Therefore, they are well recognized by body and biocompatible according to all current standards. CaP, namely, hydroxyapatite (HAp) and  $\beta$ -tricalcium phosphate ( $\beta$ -TCP), ceramics and related compounds represent the most important class of biomaterials for bone regeneration over 40 years. However, these materials have not been explored to their maximum extent yet. Recently, biogenic mineral elements have become important additives in treatments for bone regeneration and repair. Therefore, studies in bone grafting materials, particularly, CaP, have been focused on phase composition control and effects of ionic substitutions, including Mg, in order to optimize the bioresorbability and bioactivity. The importance of Mg in bone is well-known. Specifically, Mg is needed for bone formation and can also be referred to as a natural “calcium antagonist”. Thus, it is expected that partial substitution of Ca with Mg might significantly improve biological properties of the CaP. It is hypothesized that Mg-modified CaP bioceramic would ensure faster and more efficient recovery of damaged bone tissues by decomposing into environment of the body and gradually releasing  $Mg^{2+}$  ions able to act on bone diseases such as osteoporosis.

Still, there is a lack of information dealing with systematic and comparative studies concerning influence of various combinations of Mg content and HAp/ $\beta$ -TCP phase ratios on the physicochemical and biological properties of bioceramics. In the present research, considering the overall aim, which is to develop alternative implant materials for osteoporotic bone tissue regeneration, Mg-modified CaP bioceramics have been studied. Particularly, the effect of relatively low amounts, *i.e.*, bone-like amounts (up to 1 % (by weight)), of Mg containing CaP bioceramic has been investigated on *in vitro* activities of osteoblastic cells and osteogenic stem cells.

### The Aim of the Doctoral Thesis

→ To develop magnesium modified calcium phosphate bioceramics with variable and reproducible phase and chemical composition for bone defect repair.

### Tasks of the Doctoral Thesis

→ To perform literature survey in order to devise the synthesis technology for laboratory-scale preparation of magnesium modified calcium phosphates, namely, hydroxyapatite,  $\beta$ -tricalcium phosphate and biphasic calcium phosphate, bioceramics.

- To synthesize magnesium modified calcium phosphate bioceramic precursors, namely, hydroxyapatite, calcium deficient hydroxyapatite and apatitic tricalcium phosphate, by systematically changing concentration of the magnesium source in synthesis media.
- To evaluate an effect of varying magnesium content on physicochemical properties of obtained calcium phosphates products, as well as bioactivity of calcium phosphates bioceramics.
- To critically evaluate optimal magnesium content and phase composition of calcium phosphates bioceramics for bone tissue engineering applications based on the literature data and experimentally obtained results.

### **Thesis Statements**

- The modification of calcium phosphates, *i.e.*, hydroxyapatite, biphasic calcium phosphates and  $\beta$ -tricalcium phosphate, with magnesium up to  $\sim 1$  % (by weight) alters microstructure and solubility, which, in turn, reflect in the *in vitro* bioactivity of the obtained bioceramics.
- The substitution of calcium atoms with magnesium in the crystalline structure of calcium phosphates promotes the release of magnesium ions and, thus, provides adjustable bioresorption under physiological conditions and enhances cell response (*i.e.*, viability and activity) to the obtained bioceramics.

### **Scientific Significance**

- For the first time, systematic and complex studies of coherence between magnesium content, phase composition and physicochemical properties, and bioactivity of the calcium phosphates bioceramics have been performed.
- For the first time, porous magnesium containing calcium phosphates, *i.e.*, hydroxyapatite and  $\beta$ -tricalcium phosphate, bioceramics have been formed from precipitated hydroxyapatite and apatitic tricalcium phosphate powders with varying magnesium content by ammonium hydrogen carbonate provided viscous slurry foaming method.

### **Practical Significance**

- A relatively simple, low-cost, clean synthesis technique based on aqueous precipitation, which is suitable for preparation of magnesium modified calcium phosphates with variable and reproducible phase and chemical composition, has been developed.

### **Approbation of Research Results and Publications**

- The scientific achievements and main results of the Thesis have been summarised in 15 full text scientific manuscripts, and presented in 27 international conferences (32 peer-reviewed conference proceeding abstracts).

## List of Publications

1. Šalma-Ancāne, K., Stīpniece, L., Borodajenko, N., Jakovļevs, D., and Bērziņa-Cimdiņa, L. Incorporation of Magnesium Ions into Synthetic Hydroxyapatite: Synthesis and Characterization. *Key Engineering Materials*, **2012**, Vol. 527, pp. 26–31.
2. Stīpniece, L., Šalma-Ancāne, K., Jakovļevs, D., Borodajenko, N., and Bērziņa-Cimdiņa, L. The Study of Magnesium Substitution Effect on Physicochemical Properties of Hydroxyapatite. *Scientific Journal of RTU: Materials Sciences and Applied Chemistry*. **2013**, Vol. 28, pp. 51–57.
3. Stīpniece, L., Šalma-Ancāne, K., Borodajenko, N., Sokolova, M., Jakovļevs, D., and Bērziņa-Cimdiņa, L. Characterization of Mg-substituted Hydroxyapatite Synthesized by Wet Chemical Method. *Ceramics International*, **2014**, Vol. 40, Iss. 2, pp. 3261–3267.
4. Šalma-Ancāne, K., Stīpniece, L., Irbe, Z., Sokolova, M., Kriekē, G., and Bērziņa-Cimdiņa, L. Effect of Mg content on thermal stability of  $\beta$ -tricalcium phosphate ceramics. *Key Engineering Materials*, **2014**, Vol. 604, pp. 192–195.
5. Šalma-Ancāne, K., Stīpniece, L., Ločs, J., Lakevičs, V., Irbe, Z., and Bērziņa-Cimdiņa, L. The Influence of Biogenic and Synthetic Starting Materials on the Properties of Porous Hydroxyapatite Bioceramics. *Key Engineering Materials*, **2014**, Vol. 614, pp. 11–16.
6. Šalma-Ancāne, K., Stīpniece, L., Putniņš, A., and Bērziņa-Cimdiņa, L. Development of Mg-Containing Porous  $\beta$ -Tricalcium Phosphate Scaffolds for Bone Repair. *Ceramics International*, **2015**, Vol. 41, Iss. 3, Part B, pp. 4996–5004.
7. Stīpniece, L., Šalma-Ancāne, K., Putniņš, A., and Bērziņa-Cimdiņa, L. Evaluation of Sr- and/or Mg-containing Hydroxyapatite Behavior in Simulated Body Fluid. *Key Engineering Materials*, **2015**, Vol. 631, pp. 61–66.
8. Stīpniece, L., Šalma-Ancāne, K., Loča, D., and Pastare, S. Synthesis of Strontium Substituted Hydroxyapatite through Different Precipitation Routes. *Key Engineering Materials*, **2016**, Vol. 674, pp. 3–8.
9. Stīpniece, L., Šalma-Ancāne, K., Narkevica, I., Juhņeviča, I., and Bērziņa-Cimdiņa, L. Fabrication of Nanostructured Composites based on Hydroxyapatite and  $\epsilon$ -Polylysine. *Materials Letters*, **2016**, Vol. 163, pp. 65–68.
10. Stīpniece, L., Narkevica, I., Sokolova, M., Ločs, J., and Ozoliņš, J. Novel Scaffolds Based on Hydroxyapatite/Poly(Vinyl Alcohol) Nanocomposite Coated Porous  $\text{TiO}_2$  Ceramics for Bone Tissue Engineering. *Ceramics International*, **2016**, Vol. 42, pp. 1530–1537.
11. Stīpniece, L., Šalma-Ancāne, K., Rjabovs, V., Juhņeviča, I., Turks, M., Narkevica, I., and Bērziņa-Cimdiņa, L. Development of Functionalized Hydroxyapatite/Poly(vinyl alcohol) Composites. *Journal of Crystal Growth*, **2016**, Vol. 444, pp. 14–20.

12. Šalma-Ancāne, K., Stīpniece, L., and Irbe, Z. Effect of Biogenic and Synthetic Starting Materials on the Structure of Hydroxyapatite Bioceramics. *Ceramics International*, **2016**, Vol. 42, Iss. 8, pp. 9504–9510.
13. Stīpniece, L., Narkevica, I., Šalma-Ancāne, K., and Loča, D. Sr- and/or Mg- Containing Nanocrystalline Hydroxyapatite: Study from Synthesis to Calcined Products. *Key Engineering Materials*, **2016**, Vol. 721, pp. 167–171.
14. Robinson, L., Šalma-Ancāne, K., Stīpniece, L., Meenan, B.J., and Boyd, A.R. The Deposition of Strontium and Zinc Co-Substituted Hydroxyapatite Coatings. *Journal of Materials Science: Materials in Medicine*, **2016**. (submitted; ID: JMSM-D-16-00530).
15. Stīpniece, L., Narkevica, I., and Šalma-Ancāne, K. Low Temperature Synthesis of Nanocrystalline Hydroxyapatite: Effect of Mg and Sr Content. *Journal of the American Ceramic Society*, **2016**. (accepted manuscript).

### Participation in the Scientific Conferences

1. Stīpniece, L., Šalma-Ancāne, K., Borodajenko, N., Jakovļevs, D., Krieķe, G., and Bērziņa-Cimdiņa, L. Influence of Mg-Substitution on the Characteristics of Hydroxyapatite Powders. *53<sup>rd</sup> International Scientific Conference of Riga Technical University: Dedicated to the 150th Anniversary and the 1st Congress of World Engineers and Riga Polytechnical Institute / RTU Alumni: Section: Material Science and Applied Chemistry*, Latvia, Riga, 11–12 October **2012**. (poster presentation).
2. Stīpniece, L., Šalma-Ancāne, K., Borodajenko, N., Jakovļevs, D., and Bērziņa-Cimdiņa, L. Synthesis and Characterization of Magnesium-Substituted Hydroxyapatite. *ECERS Second International Conference for Students and Young Scientists on Material Processing Science*, Goergia, Tbilisi, 10–13 October **2012**. (oral presentation).
3. Šalma-Ancāne, K., Dubņika, A., Stīpniece, L., Sokolova, M., and Borodajenko, N. Synthesis Methodology and Investigation of Calcium Phosphate Biomaterials for Bone Tissue Replacement in Regenerative Medicine. *Symposium “Bioceramics and Cells for Reinforcement of Bone”*, Latvia, Riga, 18–20 October **2012**. (poster presentation).
4. Šalma-Ancāne, K., Stīpniece, L., Borodajenko, N., Jakovļevs, D., Krieķe, G., and Bērziņa-Cimdiņa, L. Mg-Substituted Hydroxyapatite Bioceramics: Formation and Properties. *Jahrestagung der Deutschen Gesellschaft für Biomaterialien*, Germany, Hamburg, 1–3 November **2012**. (poster presentation).
5. Šalma-Ancāne, K., Stīpniece, L., Borodajenko, N., Jakovļevs, D., and Bērziņa-Cimdiņa, L. Processing and Characterization of Magnesium Containing  $\beta$ -Tricalcium Phosphate Ceramics. *13<sup>th</sup> International Conference of the European Ceramic Society (ECERS 2013)*, France, Limoge, 23–27 June **2013**. (poster presentation).

6. Stīpniece, L., Šalma-Ancāne, K., Ločs, J., Jakovļevs, D., and Bērziņa-Cimdiņa, L. Control of Hydroxyapatite/Beta-Tricalcium Phosphate Ratio of Mg-Substituted Biphasic Calcium Phosphate. *Nano and Advanced Materials Workshop and Fair (NAMF 2013)*, Poland, Warsaw, 16–19 September **2013**. (poster presentation).
7. Stīpniece, L., Šalma-Ancāne, K., Ločs, J., Kriekē, G., and Bērziņa-Cimdiņa, L. Preparation and Characterisation of Magnesium-substituted Calcium Phosphate Bioceramics. *54<sup>th</sup> International Scientific Conference of Riga Technical University: Section: Material Science and Applied Chemistry*, Latvia, Riga, 14–16 October **2013**. (oral presentation).
8. Šalma-Ancāne, K., Stīpniece, L., Ločs, J., Lakevičs, V., and Bērziņa-Cimdiņa, L. The Influence of Biogenic and Synthetic Starting Materials on the Properties of Porous Hydroxyapatite Bioceramics. *25<sup>th</sup> Symposium and Annual Meeting of the International Society for Ceramics in Medicine (BIOCERAMICS 25)*, Romania, Bucharest, 7–10 November **2013**. (oral presentation).
9. Šalma-Ancāne, K., Stīpniece, L., Kriekē, G., Sokolova, M., and Bērziņa-Cimdiņa, L. Effect of Mg Content on Thermal Stability of  $\beta$ -Tricalcium Phosphate Ceramics. *22<sup>nd</sup> International Baltic Conference of Engineering Materials & Tribology (Baltmattrib 2013)*, Latvia, Riga, 14–15 November **2013**. (oral presentation).
10. Stīpniece, L., Šalma-Ancāne, K., Ločs, J., Putniņš, A., and Bērziņa-Cimdiņa, L. Influence of Various Mg Contents on Characteristics of Porous B-Tricalcium Phosphate Ceramic. *Scandinavian Society for Biomaterials 7<sup>th</sup> conference (ScSB 2014)*, Denmark, Aarhus, 26–28 March **2014**. (poster presentation).
11. Šalma-Ancāne, K., Stīpniece, L., Putniņš, A., Ločs, J., and Bērziņa-Cimdiņa, L. Porous  $\beta$ -tricalcium Phosphate Scaffolds with Sustained Therapeutic Mg Ions Release. *13<sup>th</sup> European Symposium on Controlled Drug Delivery 2014 (ESCDD 2014)*, The Netherlands, Egmond aan Zee, 16–18 April **2014**. (poster presentation).
12. Putniņš, A., Ločs, J., Šalma-Ancāne, K., and Stīpniece, L. Degradation Behaviour of Designed Sr, Mg and Non-Substituted Hydroxyapatite Granules. *The 12<sup>th</sup> Junior Euromat Conference (Junior EuroMAT)*, Switherland, Lausanne, 21–25 July **2014**. (poster presentation).
13. Stīpniece, L., Šalma-Ancāne, K., and Bērziņa-Cimdiņa, L. Comparison of Sr-substituted Hydroxyapatite Obtained of Various Precursors through Neutralization Reaction: Characterisation at the Bulk and Particle Leve (poster presentation); Šalma-Ancāne, K., Stīpniece, L., and Bērziņa-Cimdiņa, L. Low Temperature Aqueous Precipitation of Nanocrystalline Hydroxyapatite (poster presentation). *26<sup>th</sup> Annual Conference European Society for Biomaterials (ESB 2014)*, UK, Liverpool, 31 August – 3 September **2014**.
14. Stīpniece, L., Šalma-Ancāne, K., Rjabovs, V., Putniņš, A., Juhņeviča, I., Turks, M., and Bērziņa-Cimdiņa, L. Development of Hydroxyapatite/Poly(Vinyl Alcohol) Nanostructured Composites. *55<sup>th</sup> International Scientific Conference of Riga Technical University*, Latvia, Riga, 14–17 October **2014**. (oral presentation).

15. Stīpniece, L., Šalma-Ancāne, K., Putniņš, A., Narkevica, I., and Bērziņa-Cimdiņa, L. Evaluation of Sr- and/or Mg-containing Hydroxyapatite Behaviour in Simulated Body Fluid (*poster presentation*); Šalma-Ancāne, K., Stīpniece, L., Sokolova, M., Branka, M., Loča, D., and Bērziņa-Cimdiņa, L. Preparation and Characterization of Sr and Mg Containing Hydroxyapatite-Poly(Vinyl Alcohol) Microspheres for Clinical Application (*oral presentation*). *26<sup>th</sup> Symposium and Annual Meeting of the International Society for Ceramics in Medicine (BIOCERAMICS 26)*, Spain, Barcelona, 6–8 November **2014**.
16. Stīpniece, L., and Šalma-Ancāne, K. Preparation and Characterization of Sr-Containing Calcium Phosphates (*poster presentation*); Šalma-Ancāne, K., Stīpniece, L., Ločs, J., Rjabovs, V., and Bērziņa-Cimdiņa, L. Modified Poly(Vinyl Alcohol)/Hydroxyapatite Microspheres For Bone Tissue Engineering (*poster presentation*). *Unified Scientific Approaches towards Regenerative Orthopaedics And Dentistry (REDEOR 2015)*, Italy, Venice, 25–27 March **2015**.
17. Stīpniece, L., Šalma-Ancāne, K., Rjabovs, V., and Bērziņa-Cimdiņa, L. Tailoring the Degradation of Hydroxyapatite/Poly-(Vinyl Alcohol) Composites (*oral presentation*). Šalma-Ancāne, K., Stīpniece, L., Vojevodova, A., Narkevica, I., and Bērziņa-Cimdiņa, L. Design of Multifunctional Micro-Granules based on Sr-Substituted Hydroxyapatite and Poly-(Vinyl Alcohol) (*poster presentation*). *Scandinavian Society for Biomaterials 8th conference (ScSB 2015)*, Latvia, Sigulda, 6–8 May **2015**.
18. Šalma-Ancāne, K., Stīpniece, L., Ločs, J., Rjabovs, V., and Bērziņa-Cimdiņa, L. Modified Poly(Vinyl Alcohol)-Hydroxyapatite Microspheres for Bone Tissue Engineering. *European Symposium and Exhibition on Biomaterials and Related Areas (Euro BioMAT 2015)*, Germany, Veinminer, 21–22 April **2015**. (*oral presentation*).
19. Stīpniece, L., Šalma-Ancāne, K., Sigurjonsson, E.O., and Ločs, J., Preparation and in vitro evaluation of Mg-substituted biphasic calcium phosphate bioceramics for bone tissue engineering. *14<sup>th</sup> International Conference of the European Ceramic Society (ECERS 2015)*, Spain, Toledo, 21–25 July **2015**. (*oral presentation*).
20. Rjabovs, V., Stīpniece, L., Juhņeviča, I., Narkevica, I., Šalma-Ancāne, K., Bērziņa-Cimdiņa, L., and Turks, M. Microstructured Polymer/Hydroxyapatite Composite Materials. *19<sup>th</sup> European Symposium of Organic Chemistry (ESOC 2015)*, Portuguese, Lisbon, 12–16 July **2015**. (*poster presentation*).
21. Stīpniece, L., Šalma-Ancāne, K., and Loča, D. Influence of Strontium on the Synthesis and Degradation Behaviour of Biphasic Calcium Phosphate Ceramics (*poster presentation*); Šalma-Ancāne, K., Stīpniece, L., and Narkevica, I. Development of Nanostructured Composites Based on  $\epsilon$ -Polylysine and Apatite (*oral presentation*). *27<sup>th</sup> European Conference on Biomaterials (ESB 2015)*, Poland, Krakow, 30 August – 3 September **2015**.
22. Stīpniece, L., Šalma-Ancāne, K., and Loča, D. Synthesis and Characterization of Divalent Cation Substituted Calcium Phosphates. *11<sup>th</sup> Conference for Young Scientists in Ceramics*, Serbia, Novi Sad, 21–24 October **2015**. (*oral presentation*)

23. Stīpniece, L., Šalma-Ancāne, K., Loča, D., and Pastare, S. Synthesis of Strontium Substituted Hydroxyapatite Through Different Precipitation Routes. *24<sup>th</sup> International Baltic Conference ENGINEERING MATERIALS & TRIBOLOGY BALTMATRIB 2015*, Estonia, Tallinn, 5–6 November **2015**. (*oral presentation*).
24. Stīpniece, L., Šalma-Ancāne, K., Ločs, J., and Sigurjonsson, O.E. Mg Containing Biphasic Calcium Phosphate Bioceramics: Preparation and *In Vitro* Evaluation (*poster presentation*). Narkevica, I., Stīpniece, L., and Ozoliņš, J. Hydroxyapatite/Poly(Vinyl Alcohol) Nanocomposite Coated TiO<sub>2</sub> Scaffolds for Bone Tissue Engineering (*poster presentation*). *40<sup>th</sup> International Conference and Exposition on Advanced Ceramics and Composites*, USA, Daytona Beach, 24–29 January **2016**.
25. Stīpniece, L., Vecstaudža, J., Zālīte, V., Šalma-Ancāne, K., Loča, D., and Bērziņa-Cimdiņa, L. Optimization of Design and Synthesis of Calcium Phosphates for Biomedical Application (*poster presentation*). Sokolova, M., Stīpniece, L., Vojevodova, A., Mirošņikovs, A., Šalma-Ancāne, K., Ločs, J., and Bērziņa-Cimdiņa, L. Development and Characterization of Bioresorbable Composites Based on Polymers and Calcium Phosphates for Medical Application (*poster presentation*). *LU CFI 32<sup>nd</sup> scientific conference*, Latvia, Riga, 17–19 February 2016.
26. Stīpniece, L., Šalma-Ancāne, K., Narkevica, I., and Rjabovs, V. Development of Hydroxyapatite/Modified Poly(Vinyl Alcohol) Composites for Bone Tissue Engineering. *9<sup>th</sup> Annual Meeting of the Scandinavian Society for Biomaterials*, Iceland, Reykjavik, 1–3 June **2016**. (*poster presentation*).
27. Stīpniece, L., Narkevica, I., Šalma-Ancāne, K., and Bērziņa-Cimdiņa, L. Development and Characterization of Mg-Containing Hydroxyapatite, B-Tricalcium Phosphate and Biphasic Calcium Phosphate Bioceramics (*poster presentation*). Narkevica, I., Stīpniece, L., and Ozoliņš, J. Design and Characterization of Hydroxyapatite/Poly(Vinyl Alcohol) Nanocomposite Coated Titania Scaffolds for Bone Repair (*poster presentation*). *Eighteenth annual conference YUCOMAT 2016*, Montenegro, Herceg Novi, 5–10 September **2016**.

## LITERATURE REVIEW

Diseased and damaged body parts, including bones, always have been a global problem. Experts predict that 30 % of hospital beds will soon be occupied by osteoporosis patients. Moreover, statistics shows that 20 % of patients suffering from an osteoporotic fracture do not survive within first year after surgery [1]. Thus, a demand for materials to improve the quality of life concerns the innovative use of specially designed biomaterials for the repair and reconstruction of diseased or damaged bones. Over the past few decades an amazing evolution in the development of innovative implants has occurred. Among these materials, particular importance is given to bioceramics defined as the class of ceramics used for repairing and replacing diseased and damaged parts of musculoskeletal systems.

Nowadays the focus has shifted towards bone replacement and repair materials, including bioceramics, that can mimic living tissues (biomimetic) and assist in the healing process (*i.e.*, be replaced by natural bone): thus, they are bioactive, as well as bioresorbable [2]. The most widely used bioresorbable ceramics materials include calcium phosphates (CaP). The use of CaP, including hydroxyapatite (HAp) and  $\beta$ -tricalcium phosphate ( $\beta$ -TCP), as well as biphasic calcium phosphate (BCP) composed of HAp and  $\beta$ -TCP, bioceramics as scaffolds for the repair or regeneration of diseased or damaged bone tissues, is based generally on the chemical and structural similarity to the mineral component of bone, *i.e.*, biological HAp [1], [2]. Human bone consists of about ~65 % of CaP mineral. Therefore, CaP are the materials of choice to repair damaged bone. Moreover, CaP can be easily and inexpensively produced, and can be relatively easily certified for clinical use. First CaP bone graft substitutes were launched in the 1920s, but CaP biomedical research soared in the 1970s and CaP were proposed for a broad range of biomedical applications [1].

Biological HAp has variable stoichiometry and contains various different CaP phases and ionic substitutions. As such, research into bone grafting materials, particularly, CaP, has been focused on phase composition control and effects of ionic substitutions in order to optimise bioresorbability and bioactivity. A wide range of different elements have been strategically incorporated into the structure of synthetic HAp, as highlighted in Fig. 1 [3]. Moreover, biogenic mineral elements have become important additives in treatment for bone regeneration and repair. The incorporation of ions into CaP alters the crystal structure (crystallinity and crystal size) and changes properties of the material – thermal and phase stability, solubility, surface reactivity and adsorption. Consequently, modification of CaP with the biologically active elements is of great interest for developing bone graft materials with superior bioactivity [4].

The roles in the body functions, as well as biological effects of the magnesium (Mg) have promoted the development of the biomaterials based on Mg for several decades. Up to now, orthopedic applications of metallic Mg and its alloys have been exploited due to their mechanical properties and biodegradability [5]. The modification of various biomaterials has been performed through addition of biocompatible Mg compounds,

including magnesium oxide (MgO), magnesium phosphates (MgP) *etc.*, as well as through incorporation of Mg into the crystal structure of the compound, *e.g.*, CaP. Incorporation of Mg into the CaP crystal structure is important for a number of reasons; including better understanding of biomineralization processes, increase of bioactivity, and localized-targeted delivery of the ions able to act on bone diseases such as osteoporosis. Moreover, the design of new biomaterials, which exploit Mg<sup>2+</sup> ion release ability for activating bone-forming cells, is of great interest. Stimulatory effects of Mg<sup>2+</sup> ion on osteoblasts have been reported so far. Mg<sup>2+</sup> ion is well known to promote cellular adhesion onto the substrate, and is also known to enhance proliferation, differentiation, calcification and angiogenic functions.

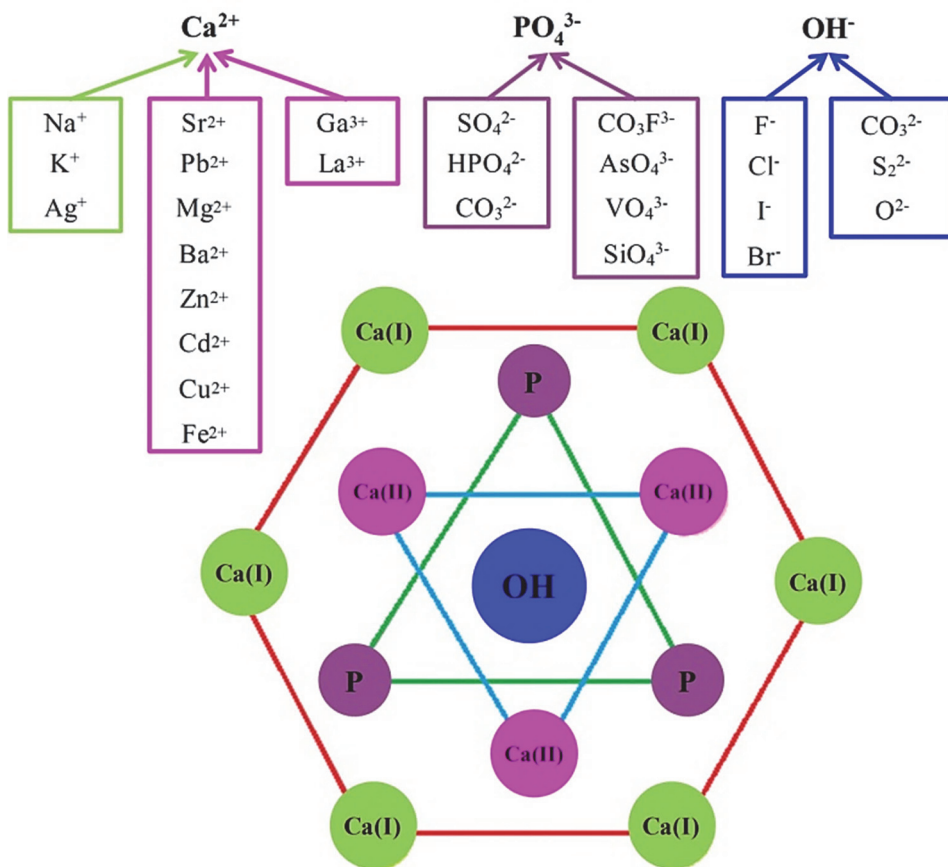


Fig. 1. Substitution possibilities in the hexagonal structure of HAp.

## EXPERIMENTAL PROCEDURE

### 1. Synthesis of Mg-Modified CaP Bioceramic Precursor Powders

The Mg-modified CaP powders with various (Ca + Mg)/P molar ratios, namely, HAp, Ca-deficient HAp (CDHAp) and apatitic-TCP (ap-TCP), were prepared via aqueous precipitation method developed at RTU Rudolfs Cimdinis Riga Biomaterials Innovation and Development Centre [6]. Various technological parameters, *i.e.*, temperature ( $T$ ) and final pH ( $pH_{final}$ ) of the synthesis mixtures, were employed to obtain products with different (Ca + Mg)/P molar ratios as illustrated in Fig. 2.

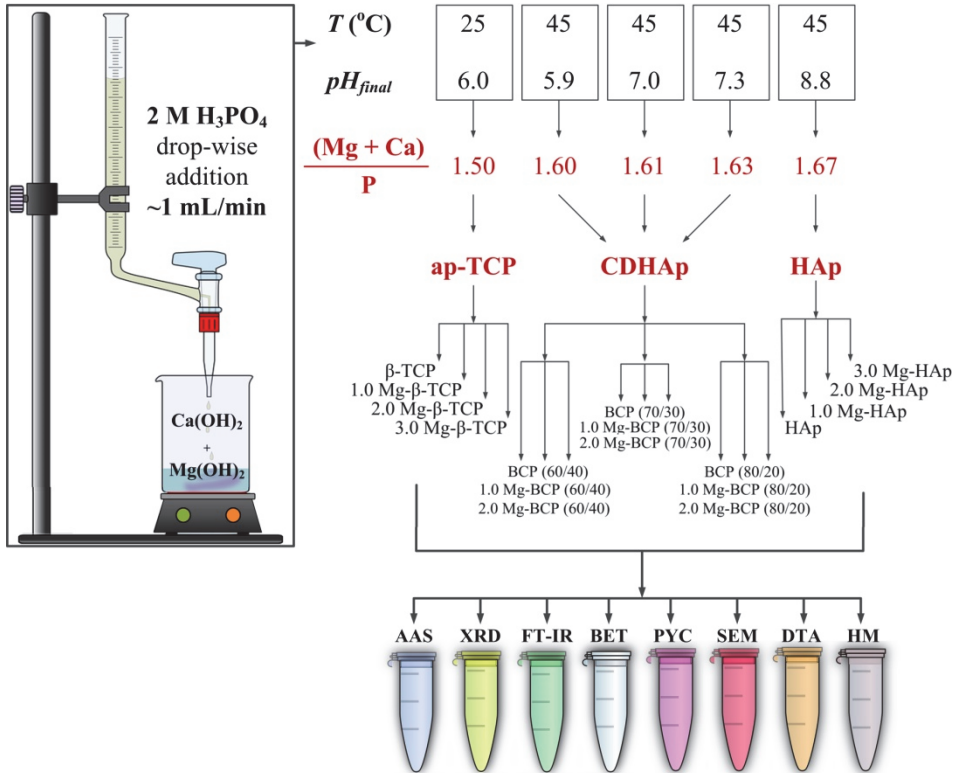


Fig. 2. Schematic representation of the Mg-modified CaP powder syntheses, presenting the technological parameters (*i.e.*,  $T$  and  $pH_{final}$ ), as well as designations of the synthesis products.

The aqueous precipitation method was modified for Mg precursor, namely MgO (*reagent-grade, ES/Scharlau*), addition into the synthesis media. Various concentrations of Mg in the products were provided by changing into synthesis media the added amount of MgO. The MgO content in the synthesis media varies from 0 % (by weight) to 3 % (by weight) in respect to a Ca source, namely CaO (*puriss., Fluka*). The main steps of the synthesis procedure:

1. Preparation of the raw materials, *i.e.*, calcinations of CaO and MgO (1100 °C, 1 h), to remove absorbed H<sub>2</sub>O and CO<sub>2</sub>.
2. Preparation of the starting suspension of Ca(OH)<sub>2</sub> or Mg(OH)<sub>2</sub>/Ca(OH)<sub>2</sub> by «lime slaking» process, *i.e.*, suspending CaO or mixture of CaO/MgO in deionized H<sub>2</sub>O.
3. Homogenization of the starting suspension by planetary ball milling (using agate grinding bowls (4 × 225 mL in volume) and balls (10 mm in diameter)) at 300 rpm for 40 min.
4. Precipitation reaction through drop-wise addition (~1 mL/min) of an aqueous solution of 2 M H<sub>3</sub>PO<sub>4</sub> (*puriss.*, *Sigma-Aldrich*) to the homogenous starting suspension of 0.15 M Ca(OH)<sub>2</sub> or Mg(OH)<sub>2</sub>/Ca(OH)<sub>2</sub> under vigorous stirring and controlled T until the required  $pH_{final}$  is reached (Fig. 2).
5. Ageing in «mother liquor» at ambient temperature for ~20 h, filtration, drying at 105 °C for 24 h and crushing of the synthesized products in a mortar, yielding powdered material, *i.e.*, the bioceramic precursor powder.

## 2. Preparation of Mg-Modified CaP Bioceramics

The Mg-modified CaP bioceramic precursor powders were used for preparation of dense and porous bioceramic scaffolds.

The synthesized powders were uniaxially compacted (10 kN) in cylindrical form of 10 mm in a diameter and sintered in air atmosphere at 1100 °C for 1 h to obtain relatively dense (hereinafter referred to as dense) Mg-modified CaP bioceramic scaffolds.

In order to prepare porous Mg-modified CaP bioceramic scaffolds, an *in situ* viscous mass foaming method was used as described in [7]. Ammonium hydrogencarbonate (NH<sub>4</sub>HCO<sub>3</sub>; purity 99–101 %, *Sigma-Aldrich*) was used as a foaming agent. The samples were sintered in air atmosphere at 1150 °C for 2 h.

## 3. Characterization Techniques

Comprehensive characterisation techniques, including Fourier transform infrared spectroscopy (FT-IR; *Varian 800 FT-IR Scimitar Series*), X-ray powder diffraction (XRD; *PANalytical X-Pert Pro*), atomic absorption spectrometry (AAS; *Varian SpektrAA 880*), were used to investigate the molecular, phase and chemical composition of the Mg-modified CaP products.

Thermal properties, which allow predicting the phase purity of the products after high-temperature treatment and assessing the effect of Mg on the CaP thermal effects and sintering behavior, were investigated by differential thermal analysis (DTA; *BÄHR Thermoanalyse DTA 703*) and dilatometric experiments by heating microscope (HM; *EMO-1750/30-K*), respectively.

Morphological and microstructural features of the synthesis products were studied using scanning electron microscopy (SEM; *TESCAN Mira/LMU Schottky*). Brunauer–Emmett–Teller (BET) method was used to determine a specific surface area (*SSA*) and mean particle size ( $d_{BET}$ ) of the bioceramic precursor powders by N<sub>2</sub> sorbometer (*Quantachrome QuadraSorb SI*). True density of the powders was measured by pycnometry (PYC; *Micromeritics AccuPyc 1330*) by averaging 99 cycles.

Total porosity of the Mg-modified CaP bioceramic scaffolds was measured according to EN 993-1:1995 standard test method using deionized water at ambient  $T$ .

#### 4. *In Vitro* Tests of Bioceramics

##### 1) Solubility

Solubility, namely, ion release of Mg-modified CaP bioceramics, was evaluated according to EN ISO 10993-14:2001. For the experiments, the bioceramic scaffolds were placed in TRIS-HCl buffer solution. TRIS-HCl solution was refreshed every 24 h during the experiment. All reacted solutions were saved for further analyses to measure  $\text{Ca}^{2+}$  and  $\text{Mg}^{2+}$  ionic concentrations. The  $\text{Ca}^{2+}$  and  $\text{Mg}^{2+}$  ion release from bioceramics was determined by complexometric titration with 0.01 M EDTA using automated titrator (*Mettler Toledo*) and Ca ion-selective electrode (Ca-ISE; *DX240 Ca-ISE*). In this study, three samples from each group were tested.

##### 2) *In Vitro* Bioactivity

It is accepted that the bioactive characteristic of scaffold biomaterials is their ability to bond with living bone through the formation of a biomimetic HAp layer on their surface both *in vitro* and *in vivo*. Thus, an *in vitro* bioactivity evaluation of Mg-modified CaP bioceramics was performed in simulated body fluid (SBF) at 37 °C using an incubator at different time points: 7 days (168 h), 21 days (504 h). Preparation of experimental samples and SBF for *in vitro* tests was performed in accordance with ISO 23317:2007 using the procedure proposed by *Kokubo et al.* In this study, three samples from each group were tested. After the predicted immersing time, the experimental samples were rinsed with deionized  $\text{H}_2\text{O}$  and dried at ambient temperature. Biomimetic HAp precipitation on surface of the scaffolds after soaking in SBF was investigated through SEM observations.

##### 3) Cytotoxicity

Cytotoxicity of Mg-modified HAp and  $\beta$ -TCP bioceramics was analysed using osteoblastic cell line *MG63-GFP*. Approximately 200 000 cells were seeded on each experimental sample and incubated at 37 °C. Cell growth dynamics in the second (after 48 h) and third (after 72 h) day was visually observed using fluorescence microscopy (*TESCAN Infinite 200<sup>®</sup> PRO*). After 72 h exposure the living cell number using DNA quantification method (*Invitrogen CyQUANT<sup>®</sup> Cell Proliferation Assay Kit, C7026*) was determined. After 72 h exposure cells were fixed on the surface of the samples, dehydrated at ethanol solutions of various concentrations and dried at ambient  $T$  for SEM observations.

Cytotoxicity of Mg-modified BCP bioceramics was analysed using osteogenic progenitor cells (*MC3T3-E1*). Approximately 20 000 cells were seeded on each experimental sample in  $\alpha$ -MEM cell culture media and incubated at 37 °C and 5 %  $\text{CO}_2$ . Cell media were replaced with fresh media on day 3 (after 72 h) of culture. After 168 h of proliferation cells/scaffolds were harvested and cytotoxicity was analysed using the MTT assay.

Results of bioceramics were compared to tissue culture plastic that acted as a control.

## RESULTS AND DISCUSSION

### 1. Characterisation of Mg-Modified CaP Precursor Powders

The main characteristics of bioceramic precursor powders are summarised in Table 1. Mg-modified CaP, *i.e.*, HAp, CDHAp and ap-TCP, containing bone-like amounts of Mg (up to 1 % (by weight) [2]) were obtained. An actual Mg content of the synthesis products measured by AAS was reported as a function of the Mg content (theoretical Mg content) in the synthesis solution.

Table 1

The Analysis of Mg Content of Synthesis Products and Mean Particle Size ( $d_{\text{BET}}$ ) of Bioceramic Precursor Powders

	Designation of the synthesis products	Theoretical Mg content, % (by weight)	Actual Mg content, % (by weight)	$d_{\text{BET}}$ , nm
<b>HAp</b>	HAp	0	$0.21 \pm 0.02$	22
	1.0 Mg-HAp	0.34	$0.43 \pm 0.09$	21
	2.0 Mg-HAp	0.68	$0.64 \pm 0.10$	21
	3.0 Mg-HAp	1.02	$0.83 \pm 0.19$	22
<b>CDHAp</b>	BCP (80/20)	0	$0.32 \pm 0.04$	28
	1.0 Mg-BCP (80/20)	0.34	$0.31 \pm 0.04$	27
	2.0 Mg-BCP (80/20)	0.68	$0.69 \pm 0.08$	26
	BCP (70/30)	0	$0.33 \pm 0.04$	28
	1.0 Mg-BCP (70/30)	0.34	$0.51 \pm 0.06$	27
	2.0 Mg-BCP (70/30)	0.68	$0.75 \pm 0.09$	23
	BCP (60/40)	0	$0.28 \pm 0.04$	32
	1.0 Mg-BCP (60/40)	0.34	$0.36 \pm 0.04$	32
	2.0 Mg-BCP (60/40)	0.68	$0.64 \pm 0.08$	29
<b>ap-TCP</b>	$\beta$ -TCP	0	$0.25 \pm 0.03$	24
	1.0 Mg- $\beta$ -TCP	0.34	$0.32 \pm 0.04$	23
	2.0 Mg- $\beta$ -TCP	0.68	$0.56 \pm 0.08$	21
	3.0 Mg- $\beta$ -TCP	1.02	$0.67 \pm 0.08$	20

In general, Mg content in the synthesis products increased upon increasing an amount of the  $\text{Mg}^{2+}$  source (*i.e.*, MgO) in the synthesis suspension. Presence of Mg (up to  $(0.33 \pm 0.04)$  % (by weight)) in the synthesis products prepared without extra MgO addition, *i.e.*, HAp, BCP (80/20), BCP (70/30), BCP (60/40) and  $\beta$ -TCP, resulted in an impurity introduced from the raw material – commercial CaO. Difference between the theoretical and the actual Mg content is an indicative that part of the raw materials remained dissolved in the synthesis solutions and was removed by filtration causing a cationic deficiency.

Phase composition and crystallinity of the synthesized powders were evaluated using XRD analysis. Phase composition analysis was based on compliance of detected XRD peaks (in the  $2\theta$  range from  $10^\circ$  to  $60^\circ$ ) with HAp phase in agreement with International Centre for Diffraction Data (ICDD) PDF-2/2005 file #01-072-1243. The XRD patterns (Fig. 3) confirmed that the main phase of the synthesis products was nanocrystalline HAp, which was characterised by low-intensity and broad diffraction peaks [8].

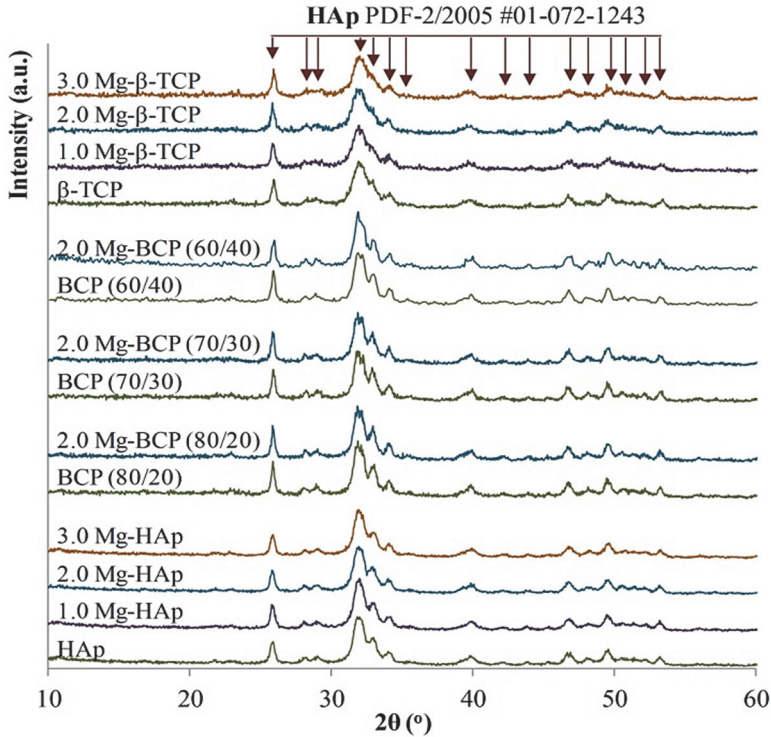


Fig. 3. XRD patterns of Mg-modified ap-TCP, CDHAp and HAp.

Physicochemical properties of bioceramic scaffolds such as porosity, grain shape and size, *etc.* that are key parameters to the evaluation of biological properties depend on the precursor powder morphology (particle size, shape and agglomeration) as it affects the sintering and grain densification. Thus, the synthesis products were collected in form of suspension and dried at  $105^\circ\text{C}$  to investigate morphology of Mg-modified CaP powders with various  $(\text{Ca} + \text{Mg})/\text{P}$  molar ratios using SEM. SEM micrographs (Fig. 4) showed a significant degree of agglomeration for all synthesis products. Thus, it is hard to distinguish between well-defined primary particles and agglomerates, *i.e.*, larger-sized secondary particles. Nevertheless, Mg-modified CaP powders appeared to have needle-like particle morphology of nanometer scale dimensions, *i.e.*, length of 150–200 nm and diameter of 25–50 nm.

In addition, mean size of the bioceramic precursor powder particles was estimated from the  $\text{N}_2$  adsorption isotherms using BET particle diameter ( $d_{\text{BET}}$ ). BET measurements indicated that *SSA* of the CaP powders exhibited higher values with increased Mg content.

Observations illustrated in Table 1 suggest that substitution of Ca with Mg into the CaP structure causes deformation of crystals resulting into reduction of mean particle size of the synthesized powders [9].

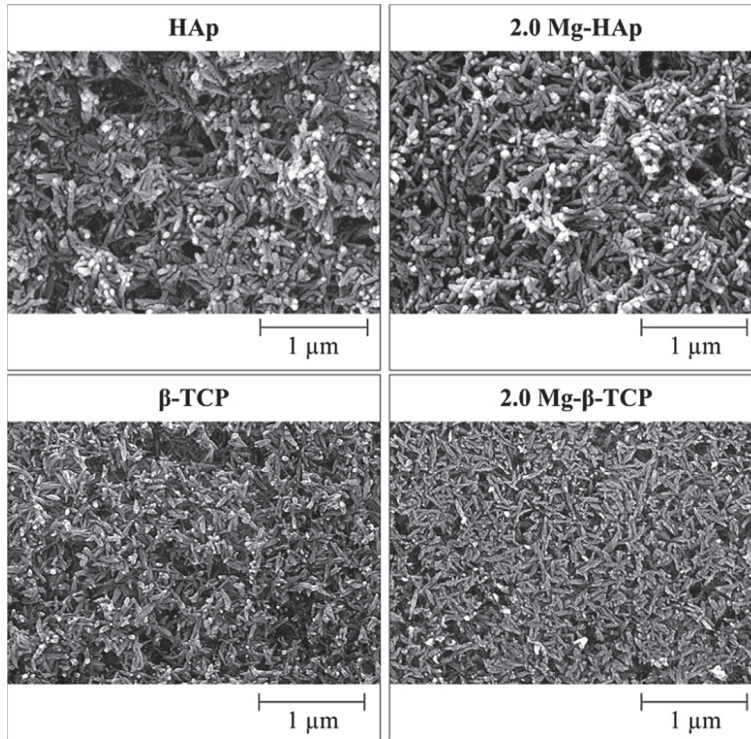


Fig. 4. SEM micrographs of the Mg-modified CaP bioceramic precursor powders.

The Mg-modified HAp, BCP and  $\beta$ -TCP bioceramic scaffolds, which were used for *in vitro* testing of biological characteristics, were obtained by sintering Mg-modified HAp, CDHAp and ap-TCP compacts at 1100 °C for 1 h, respectively. Thermal stability of bioceramic precursor powders was evaluated in order to predict phase purity of bioceramics and evaluate the effect of Mg addition on the characteristic thermal effects of the studied CaP. Moreover, the influence of Mg addition on sintering behavior of Mg-modified CaP was evaluated through dilatometric analysis by HM. Considering that solubility (ion release ability), *in vitro* bioactivity (ability to trigger formation of biomimetic HAp layer on the surface) and cytotoxicity (cell vitality and activity) are highly dependent on chemical and phase composition, as well as microstructure of the experimental samples, the aforementioned characteristics are described hereafter.

## 2. Characterisation of Mg-modified HAp Bioceramics

Influence of Mg addition on thermal effects and thermal stability of HAp phase up to 1350 °C was evaluated by DTA. The DTA curves (Fig. 5 (A)) displayed the following thermal effects:

- Endothermic effect N° 1 in the temperature region between ~50 °C and ~150 °C observed in all of the DTA curves was due to the removal of physically adsorbed H<sub>2</sub>O and CO<sub>2</sub>.
- Exothermic effect N° 2 at ~350 °C was due to the crystallization of HAp phase.

According to the literature, incorporation of Mg leads to a gradual transformation of HAp to  $\beta$ -TCP between 300 °C and 1100 °C, depending on the Mg content [10]. The DTA curves did not show any other endothermic and/or exothermic peak indicating decomposition of HAp phase. Thus, it might be suggested that HAp containing up to (0.83  $\pm$  0.19) % (by weight) of Mg was stable up to 1350 °C. However, intensity of partial HAp  $\rightarrow$   $\beta$ -TCP phase transition might be too low to be detected by DTA. Thus, the XRD analysis must be performed to confirm the phase purity of Mg-modified HAp bioceramics sintered at 1100 °C for 1 h.

Dilatometric curves summarised in Fig. 5 (B) show the sintering profile along the temperature range from 25 °C to 1350 °C for Mg-modified HAp. Regardless of the Mg content, the sintering process of Mg-modified HAp started at ~600 °C. Intensive sintering of HAp bioceramic precursor powders was observed within the temperature range from 950 °C to 1050 °C. At 1100 °C, *i.e.*, temperature used for sintering of bioceramics, the linear shrinkage of Mg-modified HAp was found to be between 45 % and 50 %. The SEM investigations of Mg-modified HAp bioceramics indicated the formation of elongated grains of heterogeneous size and shape while the content of Mg increased (Fig. 5 (C)). However, by collating SEM observations and values of the total porosity of Mg-modified HAp bioceramic scaffolds summarised in Table 2, it can be claimed that the differences were insignificant and they would not affect *in vitro* tests.

Table 2

Density and Total Porosity of Dense Mg-Modified HAp Bioceramic Scaffolds

Sample designation	Density, g/cm <sup>3</sup>	Total porosity, %
HAp	2.86 $\pm$ 0.06	9.50 $\pm$ 1.77
1.0 Mg-HAp	2.68 $\pm$ 0.06	15.24 $\pm$ 1.98
2.0 Mg-HAp	2.59 $\pm$ 0.06	18.07 $\pm$ 5.18
3.0 Mg-HAp	2.31 $\pm$ 0.08	27.05 $\pm$ 2.65

XRD analysis (Fig. 6) revealed the final composition of Mg-modified HAp bioceramics. No secondary phases such as CaO and MgO peaks were detected at least at the detection limits of the instrument (*i.e.*, concentration of ~2 % (by weight)). Accordingly, the sum of extraneous phases (CaO and MgO) was less than 5 % (by weight). Thus, the requirements of ISO 13779-3 norm were fulfilled. From the XRD analyses, it was confirmed that the single phase HAp with Mg content up to (0.64  $\pm$  0.10) % (by weight) and with maintained original crystalline structure was obtained. Thereby, it was likely to achieve substitution of Mg into the structure of synthetic HAp resembled to those of bone mineral [2]. However, the peaks derived from both HAp and  $\beta$ -TCP were detected in the XRD patterns containing (0.83  $\pm$  0.19) % (by weight) of Mg (3.0 Mg-HAp), which indicated the formation of BCP ceramics *in situ*, thus, confirming the destabilising effect of Mg on the HAp phase, *i.e.*, lowering of thermal stability of HAp, as reported in literature *de facto* [10]. It is generally difficult to distinguish between  $\beta$ -TCP and Mg-containing  $\beta$ -TCP (whitlockite) phases due to overlapping of characteristic XRD peaks. Thus, occupancy

and behavior of Mg in the biphasic mixtures cannot be determined quantitatively from the present results, which need an extensive structural investigation. Moreover, according to the measured values of total porosity (Table 2), it was observed that the scaffolds labelled as 3.0 Mg-HAp exhibited higher porosity than other Mg-modified HAp bioceramic scaffolds. Most likely, it was due to the presence of secondary phase – whitlockite.

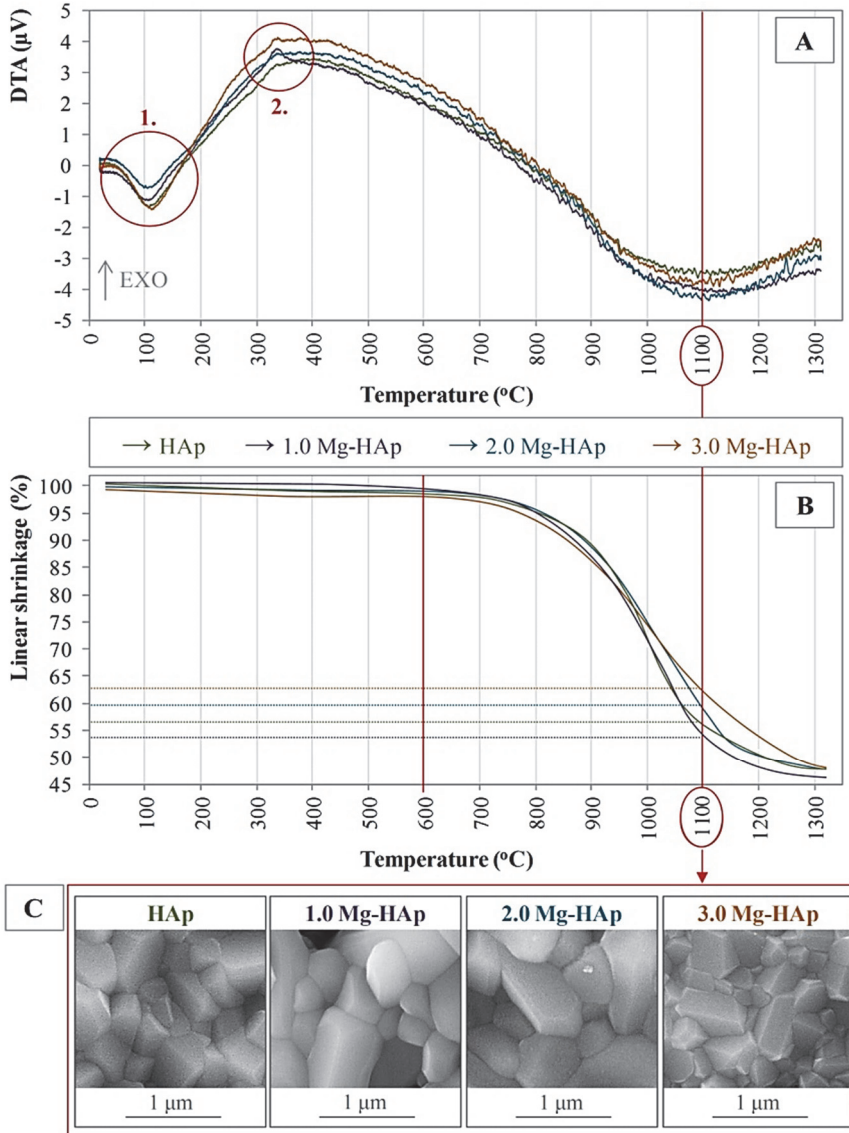


Fig. 5. A – DTA curves, B – dilatometric curves of Mg-modified HAp and C – SEM micrographs of Mg-modified HAp bioceramics sintered at 1100 °C.

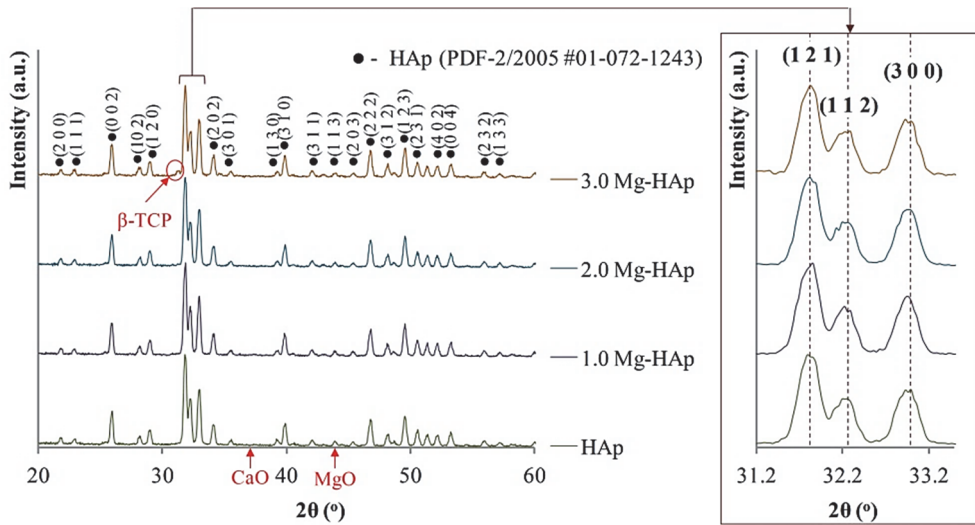


Fig. 6. XRD patterns of Mg-modified HAp bioceramics.

### 3. Characterisation of Mg-Modified $\beta$ -TCP Bioceramics

Effect of Mg addition on thermal stability of  $\beta$ -TCP phase up to 1350 °C was evaluated by DTA. The DTA curves (Fig. 7 (A)) displayed the following thermal effects:

- Endothermic effect N° 1 in the temperature region between ~50 and ~150 °C was due to the removal of physically adsorbed H<sub>2</sub>O and CO<sub>2</sub>.
- Thermal effects N° 2 within the temperature range of ~700 - ~800 °C were attributed to crystallization of  $\beta$ -TCP phase. Transformation of ap-TCP →  $\beta$ -TCP was characterised by exothermic reaction followed by endothermic reaction. *Combes et al.* have reported that the exothermic effect is attributed to particle rearrangement of low-crystallinity phases [11]. Intensity of the exothermic effect increased with Mg content. This was due to a direct proportionality between an amount of low-crystallinity phases and exothermic effect intensity [11]. Thus, narrowing of the exothermic peak at ~720 °C implied that Mg promoted formation of low-crystallinity admixture in Mg-modified ap-TCP.
- Endothermic effect N° 3 at ~1280 °C resulted from the phase transformation of  $\beta$ -TCP to  $\alpha$ -TCP. For samples with higher Mg content  $\beta$ -TCP →  $\alpha$ -TCP transition was not observed up to 1350 °C. This indicated that addition of up to (0.67 ± 0.08) % (by weight) Mg stabilised  $\beta$ -TCP phase.

Sintering of Mg-modified ap-TCP started at ~700 °C, and intensive shrinkage occurred between ~950 °C and ~1150 °C (Fig. 7 (B)). Linear shrinkage of Mg-modified ap-TCP at 1350 °C varied as follows:  $\beta$ -TCP ~45 %; 1.0 Mg- $\beta$ -TCP, 2.0 Mg- $\beta$ -TCP, 3.0 Mg- $\beta$ -TCP ~55 %. This was due to the  $\beta$ -TCP →  $\alpha$ -TCP transition at ~1280 °C as detected in the DTA curve of ap-TCP labelled as  $\beta$ -TCP. The phase transformation inhibited densification due to different grain size and shape of the present phases.

Micrographs of Mg-modified  $\beta$ -TCP bioceramics (Fig. 7 (C)) showed a significant effect of the Mg content on grain size. Namely, the increased Mg content inhibited grain growth, which resulted in the mean grain size of  $(1.4 \pm 0.5) \mu\text{m}$  for  $\beta$ -TCP bioceramics and of  $(0.5 \pm 0.1) \mu\text{m}$  for 3.0 Mg- $\beta$ -TCP bioceramics. Thus, formation of  $\beta$ -TCP bioceramics with homogenous microstructure with relatively small grains was induced by addition of Mg.

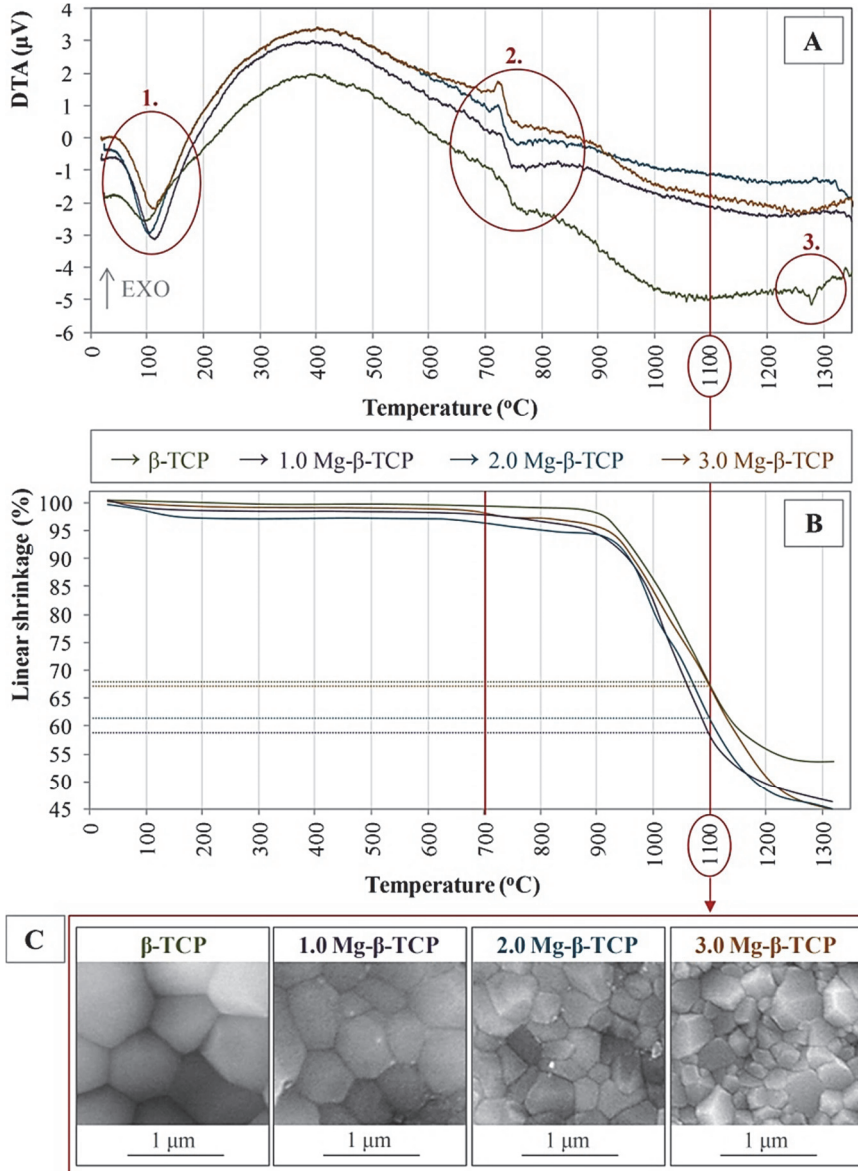
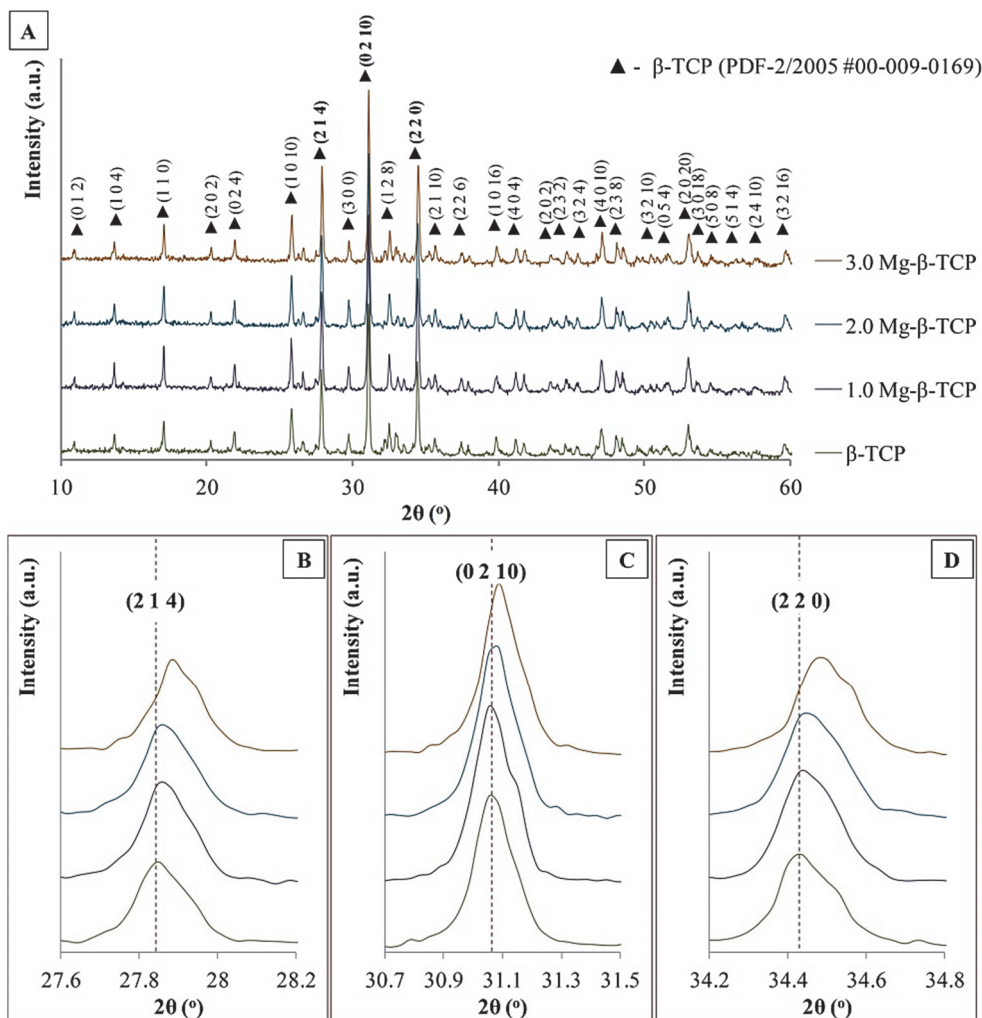


Fig. 7. A – DTA curves, B – dilatometric curves of Mg-modified  $\beta$ -TCP and C – SEM micrographs of Mg-modified  $\beta$ -TCP bioceramics sintered at 1100  $^{\circ}\text{C}$ .

Table 3

Density and Total Porosity of Dense Mg-Modified  $\beta$ -TCP Bioceramic Scaffolds

Sample designation	Density, g/cm <sup>3</sup>	Total porosity, %
$\beta$ -TCP	2.71 $\pm$ 0.02	14.36 $\pm$ 2.20
1.0 Mg- $\beta$ -TCP	2.86 $\pm$ 0.04	9.47 $\pm$ 1.57
2.0 Mg- $\beta$ -TCP	2.93 $\pm$ 0.06	7.14 $\pm$ 1.20
3.0 Mg- $\beta$ -TCP	2.94 $\pm$ 0.07	6.92 $\pm$ 0.68

Fig. 8. XRD patterns of Mg-modified  $\beta$ -TCP bioceramics.

Dilatometric results and SEM observations of Mg-modified  $\beta$ -TCP bioceramics were in good agreement with porosity measurements summarised in Table 3. The total porosity decreased while Mg content increased. Thus, it can be concluded that the increased Mg

content in ap-TCP leads to improved sintering of the powders. These results correlate with data obtained by the BET method, which suggests that Mg incorporation into the ap-TCP leads to a smaller particle size and, thus, to better sintering as expected for powder characterised by smaller and, therefore, more reactive particles [12].

XRD analyses (Fig. 8 (A)) revealed the final composition of Mg-modified  $\beta$ -TCP bioceramics. The peak positions and relative peak intensities for all of the obtained bioceramics correspond closely to those indicated in the ICDD PDF-2/2005 file #00-009-0169 for  $\beta$ -TCP. No XRD peaks corresponding to the extraneous phases such as CaO, MgO,  $\alpha$ -TCP and/or calcium pyrophosphate ( $\text{Ca}_2\text{P}_2\text{O}_7$ ) were detected, thus, fulfilling the requirements of ISO 13779-3 norm for CaP implant materials. Upon increasing Mg content in the  $\beta$ -TCP XRD peaks shifted towards higher  $2\theta$  values (Fig. 8 (B,C,D)), which confirmed Mg incorporation into  $\beta$ -TCP structure, consequently, causing crystalline lattice deformation and crystallite size reduction, as reported in the literature [13].

#### 4. Characterisation of Mg-Modified BCP Bioceramics

Dilatometric curves summarised in Fig. 9 show the sintering of Mg-modified CDHAp powders along the temperature range from 25 °C to 1350 °C. It was proven that an increase of Mg content promoted a two-step sintering process. For the samples BCP (80/20) and BCP (70/30), the shrinkage occurred in one step beginning at  $\sim 600$  °C. The shrinkage of the samples 2.0 Mg-BCP (80/20) and 2.0 Mg-BCP (70/30) occurred in two steps. Differences among the samples are attributed to structural changes associated with various incorporation levels of Mg. The first sintering step starting at  $\sim 600$  °C is attributed to particle rearrangement further to a better crystallization. The first sintering step reached a maximum at  $\sim 950$  °C and overlapped with the second step corresponding to a major densification. The linear shrinkage of the samples after heating up to 1100 °C was approximately  $(30 \pm 5)$  %.

XRD analysis of Mg-modified BCP confirmed the formation of biphasic, *i.e.*, HAp and  $\beta$ -TCP mixtures (Fig. 10). Moreover, the increase of  $\beta$ -TCP content in respect to HAp was found to be directly proportional to the level of Ca-deficiency in the CDHAp powders. The BCP bioceramics with the increased Mg content exhibited slightly higher portion of  $\beta$ -TCP phase. It can be inferred that incorporation of Mg generated formation of  $\beta$ -TCP as a secondary phase. It was demonstrated that incorporation of Mg sensibly affected HAp crystallization and its thermal stability promoting formation of  $\beta$ -TCP phase and, thus, forming BCP mixtures *in situ* [10]. However, occupancy and behaviour of Mg in the biphasic mixtures cannot be determined quantitatively from the present results, which need an extensive structural analysis.

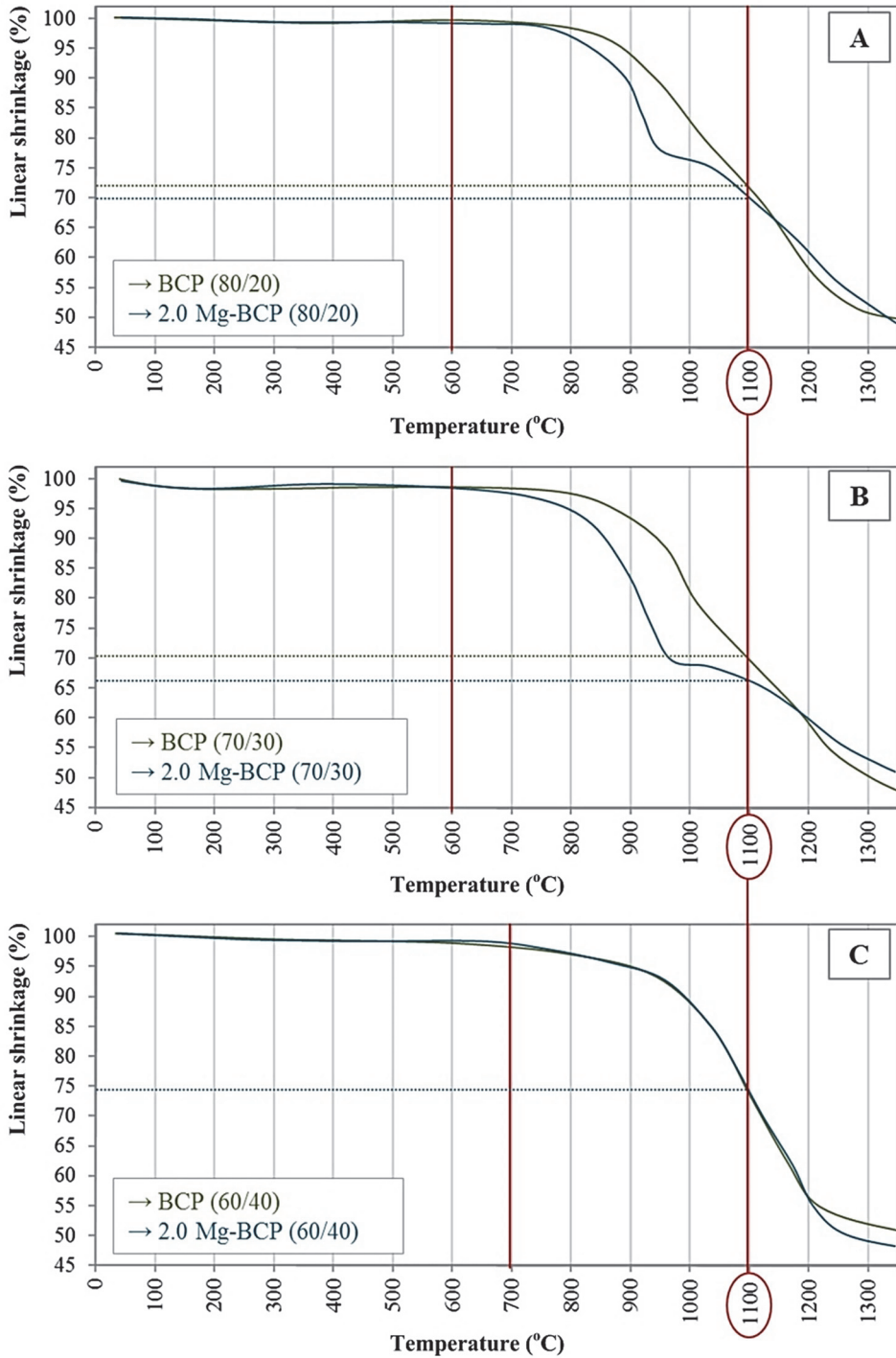


Fig. 9. Dilatometric curves of Mg-containing CDHAp with (Mg + Ca)/P molar ratio A – 1.63, B – 1.61 and C – 1.60.

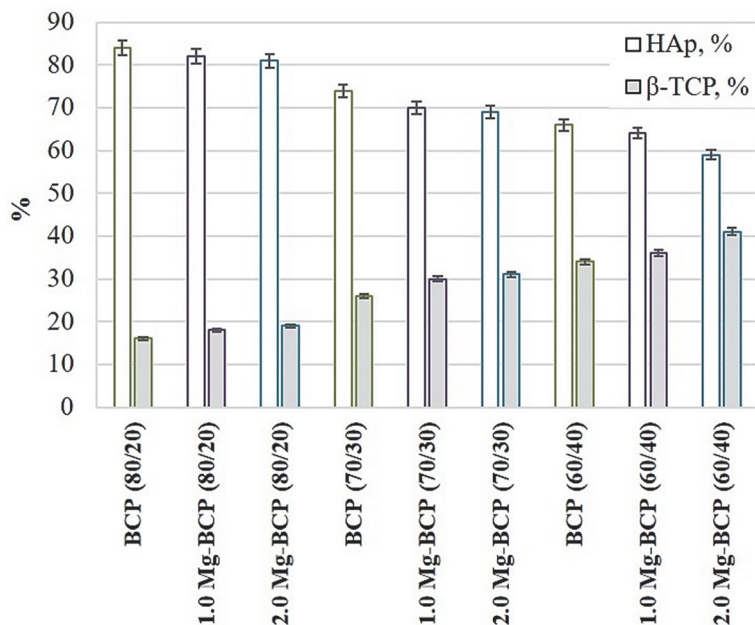


Fig. 10. Actual percentage of HAp and  $\beta$ -TCP content of Mg-modified BCP bioceramics.

## 5. Solubility, *In Vitro* Bioactivity and Cytotoxicity of Mg-Modified CaP Bioceramics

The release of  $\text{Ca}^{2+}$  and  $\text{Mg}^{2+}$  ions from Mg-modified CaP bioceramics was estimated to support its bioresorbability. An ability of Mg-modified CaP bioceramics to simultaneously release  $\text{Ca}^{2+}$  and  $\text{Mg}^{2+}$  ions was evaluated through immersing the samples in TRIS-HCl buffer solution and measuring the released  $\text{Ca}^{2+}$  and  $\text{Mg}^{2+}$  ion concentrations every 24 h. The provided tests are primarily the analysis of the initial dissolution and not as much the concentration of dissolved species. This reflects our opinion that the dissolution *in vivo* is not the one into a constant volume of fluid, but that ions, once dissolved, can be transported with the fluid flow away from the site of dissolution. The initial dissolution data may have the application in the interpretation of the initial events after implantation [14].

As illustrated in Fig. 11, throughout the evaluation period of 168 h  $\text{Ca}^{2+}$  and  $\text{Mg}^{2+}$  ion release from Mg-modified HAp was higher for the samples with increased Mg content, which could be attributed to better solubility of the materials. The obtained results suggest that the  $\text{Ca}^{2+}$  ion release seems to be linked to  $\text{Mg}^{2+}$  ion release. As expected,  $\text{Mg}^{2+}$  ion concentration in the experimental solution increased upon increasing Mg content in HAp bioceramics (Fig. 11 (B)).

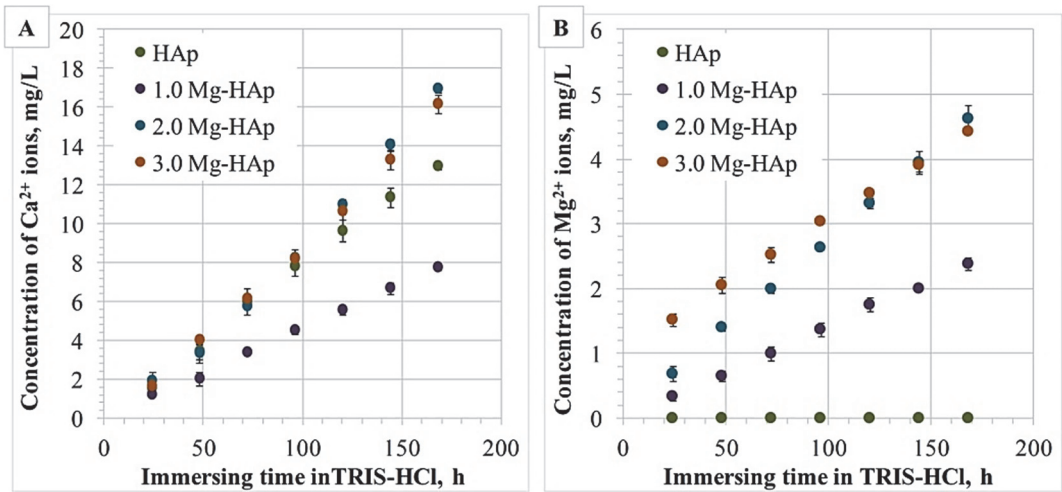


Fig. 11. Release of A – Ca<sup>2+</sup> ions and B – Mg<sup>2+</sup> ions from Mg-modified HAp bioceramics.

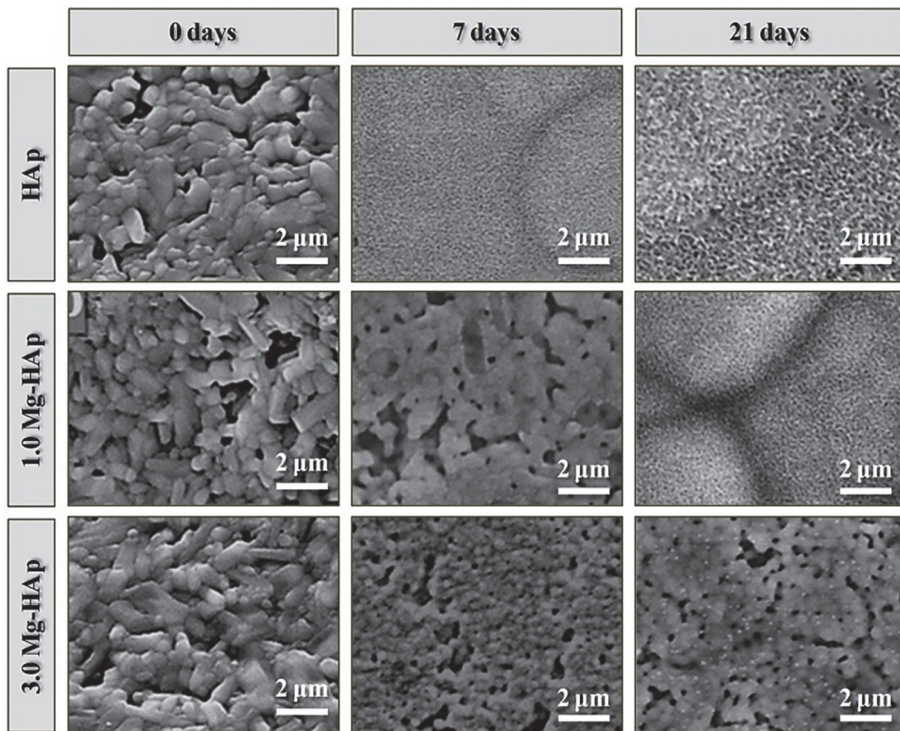


Fig. 12. SEM micrographs of Mg-modified HAp bioceramic scaffold surfaces before and after immersing in SBF for 7 and 21 days.

The ability to trigger the formation of biomimetic HAP on the surface from a close to physiological solution *in vitro* has been widely used to imply the bioactivity of bioceramics *in vivo*. Thus, *in vitro* bioactivity tests through immersing of Mg-modified CaP bioceramic scaffolds in the SBF were performed.

SEM micrographs proved morphological changes on Mg-modified HAP bioceramic scaffold surfaces after immersing in the SBF (Fig. 12). The newly formed layer had the morphology of spherulites of plate-like crystallites. After immersing for 7 days, a layer of the newly formed material covered nearly the whole surface of the HAP bioceramic scaffolds and nucleation of the new material was observed on the 1.0 Mg-HAP, 3.0 Mg-HAP bioceramic scaffolds. Continuation of growth of the plate-like crystallites on surface of HAP bioceramics after immersing in the SBF for 21 days was observed. Relatively well-distinguished spherulites were visible on the 1.0 Mg-HAP surfaces after 21 days. In turn, although the microstructural features of 3.0 Mg-HAP surface were hard to distinguish, it was proven that the newly formed compound was in low-crystalline or amorphous state. In general, it was accepted that the newly precipitated material was biomimetic HAP as a consequence of the SBF solution composition, and the fact that HAP was the most stable substance in the pH of interest (7.40) [15].

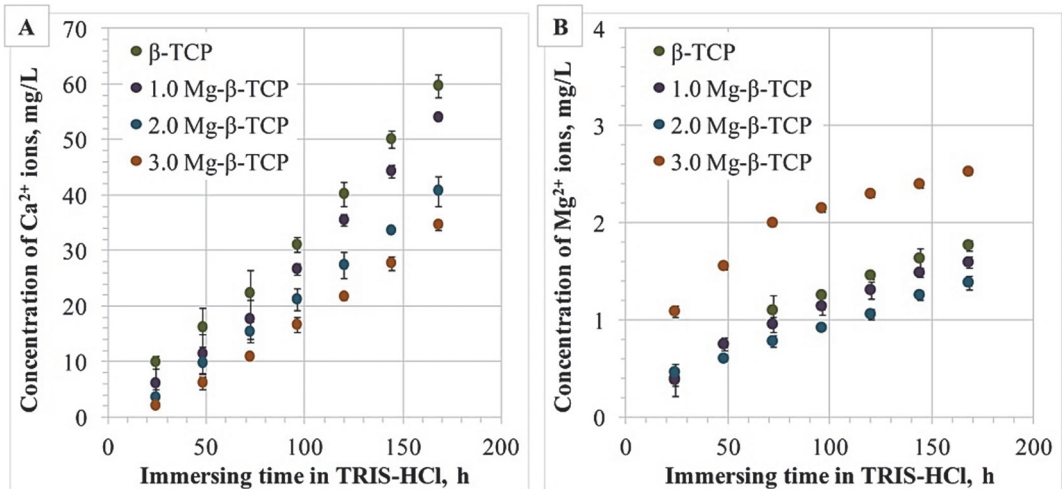


Fig. 13. Release of A – Ca<sup>2+</sup> ions and B – Mg<sup>2+</sup> ions from Mg-modified  $\beta$ -TCP bioceramics.

Solubility test results of Mg-modified  $\beta$ -TCP bioceramics illustrated in Fig. 13 showed that Mg<sup>2+</sup> ion release behavior is linked to Ca<sup>2+</sup> ions. In general, the release of Ca<sup>2+</sup> and Mg<sup>2+</sup> ions from  $\beta$ -TCP bioceramics decreased with an increase in Mg content up to (0.56 ± 0.08) % (by weight). This is indicative that modification with Mg stabilises  $\beta$ -TCP phase, *i.e.*, reduces its solubility. Up to 168 h, the 3.0 Mg- $\beta$ -TCP with the increased Mg content showed significantly enhanced Mg<sup>2+</sup> release rate in comparison with other Mg-modified  $\beta$ -TCP bioceramic scaffolds. Taking into account that Ca atom substitution by Mg in the CaP structure is limited due to differences of Ca and Mg atomic radius, it

could be estimated that reaching  $(0.67 \pm 0.08)$  % (by weight) Mg did not hold a solid position in  $\beta$ -TCP structure. Consequently,  $Mg^{2+}$  ions can be relatively easily released [13].

According to the SEM observation, the formation ability of biomimetic HAp on the surface of 2.0 Mg- $\beta$ -TCP, 3.0 Mg- $\beta$ -TCP bioceramic scaffolds was highest among Mg-modified  $\beta$ -TCP bioceramic scaffolds (Fig. 14). This is due to lower solubility of  $\beta$ -TCP bioceramics containing a higher amount of Mg (Fig. 13).

It is possible to conclude that *in vitro* bioactivity of Mg-modified CaP bioceramics is inhibited by  $Ca^{2+}$  and  $Mg^{2+}$  ion release and *vice versa*. Supposedly, dissolution of bioceramics and precipitation of the biological HAp occur at the same time.

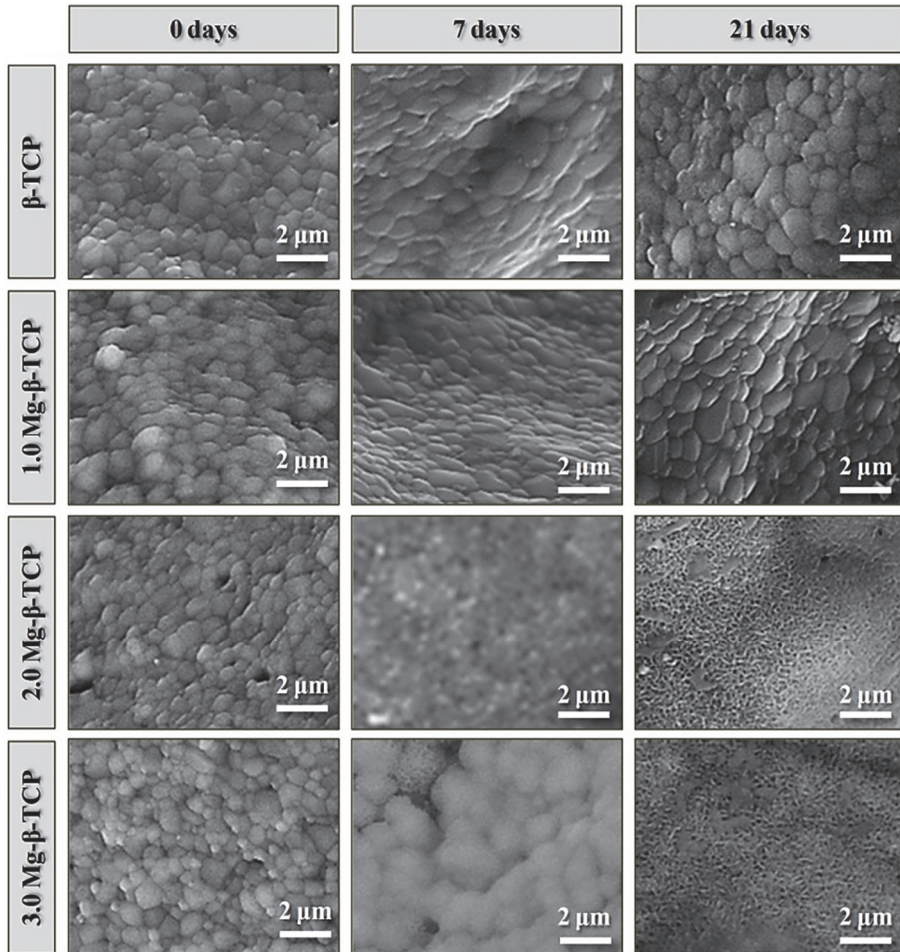


Fig. 14. SEM micrographs of Mg-modified  $\beta$ -TCP bioceramic scaffold surfaces before and after immersing in SBF for 7 and 21 days.

To evaluate the cytotoxicity of the obtained bioceramics, an assessment of osteoblast cell *MG63-GFP* proliferation on Mg-modified HAp and  $\beta$ -TCP bioceramics was evaluated. The results are shown in Fig. 15.

After exposure of Mg-modified HAp bioceramics for 72 h living osteoblastic cell *MG63-GFP* number was similar for all compositions (Fig. 15 (A)). Although the living cell number is lower than in case of the control (cell culture plate without sample), the increased cell number compared to the seeded cell number, *i.e.*, of >200 000, was observed. Thus, osteoblastic cells *MG63-GFP* showed vitality trend confirming non-cytotoxicity of Mg-modified HAp and  $\beta$ -TCP.

Mg-modified  $\beta$ -TCP bioceramics exhibited moderate cytotoxicity (Fig. 15(B)). However, conflicting results were obtained. In case of  $\beta$ -TCP bioceramics, the increased osteoblastic cell *MG63-GFP* number after 72 h of exposure was observed in comparison with the seeded cell number, *i.e.*, >200 000. By contrast, for 1.0 Mg- $\beta$ -TCP bioceramics after 72 h exposure approximately the same living cell number as seeded on bioceramics was observed. Meanwhile, 2.0 Mg- $\beta$ -TCP bioceramics showed a cytotoxic response, *i.e.*, decrease in living cell number compared to the seeded cells was promoted.

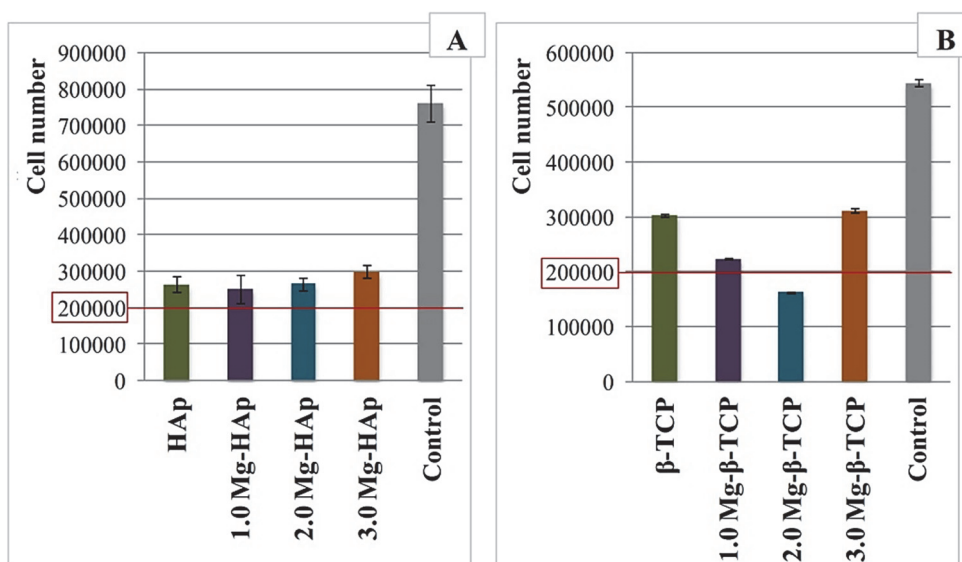


Fig. 15. Number of living osteoblastic cells in the culture media after exposure of A – Mg-modified HAp and B – Mg-modified  $\beta$ -TCP bioceramics for 72 h.

Moreover, the results showed that Mg-modified HAp and  $\beta$ -TCP bioceramics with an enhanced  $Mg^{2+}$  ion release, *i.e.*, 3.0 Mg-HAp (Fig. 11 (B)) and 3.0 Mg- $\beta$ -TCP (Fig. 13 (B)) had the most pronounced cell proliferation stimulating characteristics among other tested bioceramic scaffolds. Thus, the results indicated the positive effect of  $Mg^{2+}$  ions on osteoblastic cell *MG63-GFP* activity.

SEM micrographs showed triangular tailed morphology of the osteoblastic cells *MG63-GFP* formed by extending filopodia to adhere to Mg-modified CaP bioceramic surface (Fig. 16). No significant changes of the cell morphology were observed for various compositions suggesting that ions released into cell culture media were the main responsible factor related to alterations of Mg-modified CaP biocompatibility.

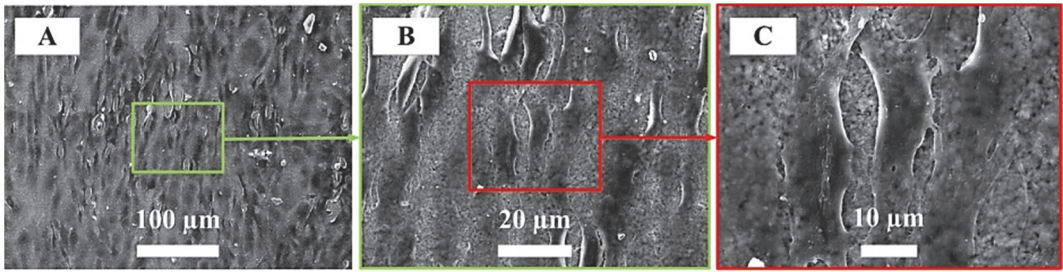


Fig. 16. SEM micrographs of osteoblasts *MG63-GFP* morphology on the Mg-modified CaP bioceramic scaffolds at various amplification (A – 500, B – 2000, C – 5000 times).

Also, the present study involved the evaluation of various combinations of HAp and  $\beta$ -TCP phase ratios and Mg content of Mg-modified BCP bioceramic on the vitality and activity of osteogenic progenitor stem cells *MC3T3-E1*. The obtained results suggested that after exposure for 168 h Mg-modified BCP bioceramics showed moderate cytotoxicity (Fig. 17). At the highest content, *i.e.*, ~70 % and ~80 %, HAp content better cell viability was observed for BCP bioceramics containing lower Mg levels. By contrast, enhanced cell activity with the increased Mg content was achieved for BCP bioceramics with the lowest, *i.e.*, ~60 %, HAp content.

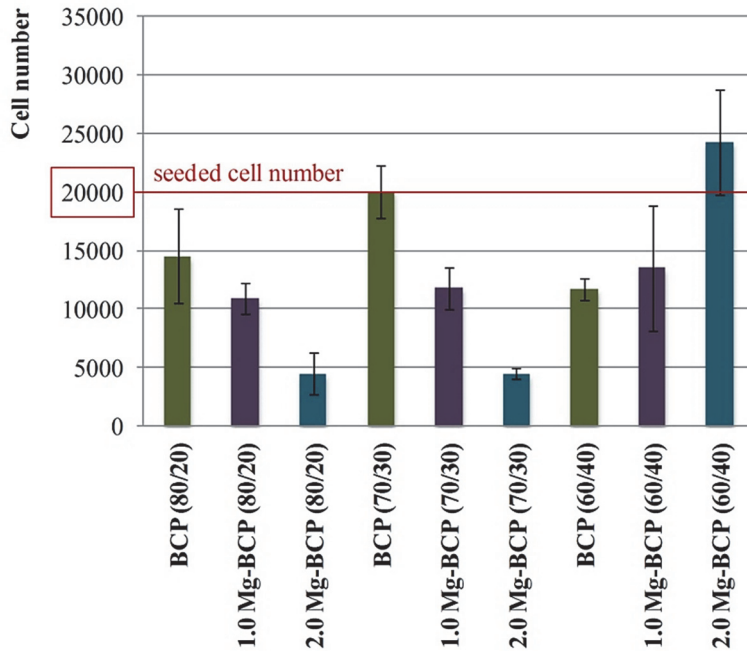


Fig. 17. Number of living osteogenic stem cells in the culture media after exposure of Mg-modified BCP bioceramics for 168 h.

## CONCLUSIONS

1. Systematic research has demonstrated that calcium phosphates with reproducible and variable phase and chemical composition can be obtained through adapted aqueous chemical precipitation method, which has been modified to successfully add magnesium source, namely, magnesium oxide, into the synthesis environment, and, consequently, incorporate magnesium in the structure of the synthesis products.
2. Thermal stability of the synthesized hydroxyapatite and apatitic tricalcium phosphate is dependent on magnesium content in the products. Increasing magnesium up to  $(0.83 \pm 0.19)$  % (by weight) lowers thermal stability of hydroxyapatite promoting partial phase transformation to  $\beta$ -tricalcium phosphate. Even a relatively small increase in the content of magnesium in the range from  $(0.25 \pm 0.03)$  % (by weight) to  $(0.67 \pm 0.08)$  % (by weight) significantly increases thermal stability of  $\beta$ -tricalcium phosphate, *i.e.*, the unmodified and magnesium modified  $\beta$ -tricalcium phosphate is stable up to 1280 °C and 1350 °C, respectively. Increase in the magnesium content of calcium deficient hydroxyapatite precursors leads to higher content of  $\beta$ -tricalcium phosphate phase in biphasic calcium phosphate bioceramics.
3. Increase of magnesium in the structure of hydroxyapatite, calcium deficient hydroxyapatite and apatitic tricalcium phosphate contributes to a specific surface area increase of  $(9 \pm 2)$  % and to a mean particle size decrease, which in turn affects the sintering processes, *i.e.*, the particle densification, and the microstructure of bioceramic after high-temperature processing. It has been found that the presence of magnesium substantially hinders  $\beta$ -tricalcium phosphate grain growth.
4. *In vitro* bioactivity, *i.e.*, biomimetic hydroxyapatite deposition on a magnesium modified hydroxyapatite and  $\beta$ -tricalcium phosphate bioceramic surface from simulated body fluid, depends on the magnesium content in the bioceramic samples. In case of hydroxyapatite bioceramics, magnesium impedes deposition of biomimetic hydroxyapatite relating to the increased solubility of hydroxyapatite induced by modification with magnesium. Biomimetic hydroxyapatite deposition on  $\beta$ -tricalcium phosphate bioceramic surface is promoted by the increasing magnesium content, which is associated with magnesium stabilising effect on  $\beta$ -tricalcium phosphate phase.
5. *In vitro* cytotoxicity tests have proven that the magnesium modified calcium phosphate bioceramic is a perspective biomaterial for bone regeneration and shows a moderate cytotoxic reaction. Magnesium modified hydroxyapatite bioceramics, regardless of the magnesium content, has shown osteoblastic cell activity.  $\beta$ -tricalcium phosphate bioceramics with a magnesium content of  $(0.67 \pm 0.08)$  % (by weight) has shown better osteoblastic cell viability compared to the unmodified  $\beta$ -tricalcium phosphate bioceramics.  $\beta$ -tricalcium phosphate content increase up to 40 % (by weight) and magnesium increase up to  $(0.64 \pm 0.08)$  % (by weight) of biphasic calcium phosphate bioceramic greatly enhanced activity of the osteogenic stem cells compared to bioceramic with lower  $\beta$ -tricalcium phosphate content and admissible magnesium content.

## REFERENCES

- [1] Habraken, W., Habibovic, P., Epple, M., and Bohner, M. (2016). Calcium phosphates in biomedical applications: Materials for the future? *Materials Today*, Vol. 19(2), pp. 69–86.
- [2] Hench, L.L. (1998). Bioactive materials: The potential for tissue regeneration. *Journal of Biomedical Materials Research*, Vol. 41, pp 511–518.
- [3] Stotzel, C., Muller, F.A., Reiert, F., Niederdraenk, F., Barralet, J.E., and Gbureck, U. (2009). Ion adsorption behaviour of hydroxyapatite with different crystallinities. *Colloids and Surfaces B*, Vol. 74(1), pp. 91–95.
- [4] LeGeros, R.Z. Calcium phosphates in oral biology and medicine. (1990). *Monographs in Oral Science*, Vol. 15, pp. 1–201.
- [5] Walker, J., Shadanbaz, S., Woodfields, T.B.F., Staiger, M.P., and Dias, G.J. (2014). Magnesium biomaterials for orthopaedic application: A review from a biological perspective. *Journal of Biomedical Materials Research Part B*, Vol. 102, pp.1316–1331.
- [6] Šalma-Ancāne, K. (2011). *Influence of calcium phosphate synthesis parameters on properties of bioceramics*. Summary of the Doctoral Thesis. Riga: RTU, 29 p.
- [7] Locs, J., Zalite, V., Berzina-Cimdina, L., and Sokolova, M. (2013). Ammonium hydrogen carbonate provided viscous slurry foaming – a novel technology for the preparation of porous ceramics. *Journal of the European Ceramic Society*, Vol. 33, pp. 3437–3443.
- [8] Drouet, C. (2013). Apatite formation: Why it may not work as planned, and how to conclusively identify apatite compounds. *BioMed Research International*, Article ID 490946, 12 p.
- [9] Ren, F., Leng, Y., Xin, R., and Ge, X. (2010). Synthesis, characterization and *ab initio* simulation of magnesium-substituted hydroxyapatite. *Acta Biomaterialia*, Vol. 6(7), pp. 2787–2796.
- [10] Stipniece, L., Salma-Ancane, K., Borodajenko, N., Sokolova, M., Jakovlevs, D., and Berzina-Cimdina, L. (2014). Characterization of Mg-substituted hydroxyapatite synthesized by wet chemical method. *Ceramics International*, Vol. 40(2), pp. 3261–326.
- [11] Combes, C., and Rey, C. (2010). Amorphous calcium phosphates: Synthesis, properties and uses in biomaterials. *Acta Biomaterialia*. Vol. 6(9), pp. 3362–3378.
- [12] Ramesh, S., Aw, K.L., Tolouei, R., Amiriyani, M., Tan, C.Y., and Hamdi, M. (2013). Sintering properties of hydroxyapatite powders prepared using different methods. *Ceramics International*, Vol. 39(1), pp. 111–119.
- [13] Ryu, H.S., Hong, K.S., Lee, J.K., and Kim, D.J. (2006). Variations of structure and composition in magnesium incorporated hydroxyapatite/ $\beta$ -calcium phosphate. *Journal of Materials Research*, Vol. 21(2), 428–436.
- [14] Kokubo, T., and Takadama, H. (2006). How useful is SBF in predicting *in vivo* bone bioactivity? *Biomaterials*, Vol. 27(15), pp. 2907–2915.
- [15] Pan, H., Zhao, X., Darvell, B.W., and Lu, W.W. (2010). Apatite-formation ability – predictor of bioactivity? *Acta Biomaterialia*, Vol. 6(11), pp. 4181–4188.